

STATISTICAL METHODS FOR EXTRACTING INFORMATION
FROM THE RAW ACCELEROMETRY DATA AND THEIR
APPLICATIONS IN PUBLIC HEALTH RESEARCH

William Farris Fadel

Submitted to the faculty of the University Graduate School

in partial fulfillment of the requirements

for the degree

Doctor of Philosophy

in the Department of Biostatistics,

Indiana University

June 2017

Accepted by the Graduate Faculty, Indiana University, in partial fulfillment of the requirements for the degree of Doctor of Philosophy.

Jaroslav Harezlak, Ph.D., Chair

Doctoral Committee

Xiaochun Li, Ph.D.

Constantin T. Yiannoutsos, Ph.D.

January 19, 2017

Andrea K. Chomistek, Sc.D.

© 2017

William Farris Fadel

DEDICATION

To my parents (Douglas and Janice Fadel), my loving wife (Amanda Fadel), and my amazing children (William Robert and Emma Rose Fadel)

ACKNOWLEDGMENTS

I would like to express my sincere gratitude to my advisor Dr. Jaroslaw Harezlak for his consistent encouragement, guidance, and patience throughout my journey towards completing my research. I have truly enjoyed the opportunity to work and grow with you these past few years. I would also like to thank the other members of my committee, Dr. Xiaochun Li, Dr. Constantin Yiannoutsos, and Dr. Andrea Chomistek for your perspective and evaluations of my dissertation research.

I have thoroughly enjoyed my time studying in this department, and I look forward to continuing collaborations with the wonderful people I have met along the way. I would also like to acknowledge the administrative staff in our department, Shari Stansbery, Ann Lyon, Cynthia Warburton, and Rhonda Byers. They were always willing to help with any problem and have made me feel like a part of the department since day one.

Finally, I would like to thank my wonderful parents, Doug and Janice Fadel, for their unwavering support through my academic life and my loving wife, Amanda, and our amazing children, William Robert and Emma Rose, for their patience with me these past few years as I have tried to complete my degree. I could have never reached this point without all of you.

William Farris Fadel

William Farris Fadel

STATISTICAL METHODS FOR EXTRACTING INFORMATION FROM THE
RAW ACCELEROMETRY DATA AND THEIR APPLICATIONS IN PUBLIC
HEALTH RESEARCH

Various methods exist to measure physical activity (PA). Subjective methods, such as diaries and surveys are relatively inexpensive ways of measuring one's PA; however, they are riddled with measurement error and bias due to self-report. Wearable accelerometers offer a noninvasive and objective measure of subjects' PA and are now widely used in observational and clinical studies. Accelerometers record high frequency data and produce an unlabeled time series at the sub-second level. An important activity to identify from such data is walking, since it is often the only form of exercise for certain populations. While much work has been done to advance the use of accelerometers in public health research, methodology is needed for quantifying the physical characteristics of different types of PA from the raw signal. In my dissertation, I advance the accelerometry research methodology in a three-paper sequence. The first paper is a novel application of functional linear models to model the physical characteristics of walking. We emphasize the signal processing used to prepare the data for analyses, and we apply the methods to a motivating dataset collected in an elder population. The second paper addresses the classification of PA. We designed an experiment and collected the data with the purpose of extracting useful and interpretable features for differentiating among walking, descending stairs, and ascending stairs. We build subject-specific classification models utilizing a tree-

based classifier. We evaluate the effects of sensor location and tuning parameters on the classification rate of these models. The third paper addresses the classification of walking types at the population level. We propose a robust normalization of features extracted for each subject and compare the model classification results to evaluate the effect of feature normalization. In summary, this work provides a framework for better use of accelerometers in the study of physical activity.

Jaroslav Harezlak, Ph.D., Chair

TABLE OF CONTENTS

LIST OF TABLES	x
LIST OF FIGURES	xii
Chapter 1 Introduction	1
Chapter 2 Functional Linear Models to Detect Associations between Char- acteristics of Walking and Health Indicators using Accelerometry Data	4
2.1 Introduction	4
2.2 Data collection and pre-processing	8
2.3 Statistical Methods	10
2.3.1 Estimation of Parameters	10
2.4 DECOS Example	14
2.5 Discussion	17
Chapter 3 Differentiating Between Walking and Stair Climbing Using Ac- celerometry Data	20
3.1 Introduction	20
3.2 Methods	25
3.2.1 Data collection and labelling	25
3.2.2 Signal processing and feature extraction	27
3.2.3 Modeling	32
3.3 Results	34
3.3.1 Model evaluation	36
3.3.2 Feature evaluation	38

3.4	Discussion	40
3.5	Acknowledgements	42
Chapter 4 Population Level Classification of Walking and Stair Climbing		
	Using Accelerometry Data	43
4.1	Introduction	43
4.1.1	Data	44
4.1.2	Proposed methods	47
4.1.3	Literature	48
4.2	Signal processing	49
4.2.1	Frequency domain features	51
4.2.2	Time domain features	55
4.3	Methods	55
4.3.1	Feature normalization	55
4.3.2	Classification model	56
4.4	Results	58
4.5	Discussion	64
4.6	Acknowledgements	65
	Appendix 4.A Final population trees and CV confusion matrices	66
Chapter 5 Discussion		
	BIBLIOGRAPHY	80
CURRICULUM VITAE		

LIST OF TABLES

2.1	Algorithm 1	11
3.1	Study Demographics	26
3.2	LS means of sensitivity for sensor location by activity.	36
3.3	LS means of sensitivity for window length by activity.	37
3.4	LS means of sensitivity for sensor location.	37
3.5	LS means of sensitivity for window length.	37
4.1	Classification results based on data collected at the hip and features extracted using 2.56 second windows.	66
4.2	Classification results based on data collected at the hip and features extracted using 5.12 second windows.	67
4.3	Classification results based on data collected at the hip and features extracted using 10.24 second windows.	68
4.4	Classification results based on data collected at the left wrist and fea- tures extracted using 2.56 second windows.	69
4.5	Classification results based on data collected at the left wrist and fea- tures extracted using 5.12 second windows.	70
4.6	Classification results based on data collected at the left wrist and fea- tures extracted using 10.24 second windows.	71
4.7	Classification results based on data collected at the left ankle and fea- tures extracted using 2.56 second windows.	72

4.8	Classification results based on data collected at the left ankle and features extracted using 5.12 second windows.	73
4.9	Classification results based on data collected at the left ankle and features extracted using 10.24 second windows.	74
4.10	Classification results based on data collected at the right ankle and features extracted using 2.56 second windows.	75
4.11	Classification results based on data collected at the right ankle and features extracted using 5.12 second windows.	76
4.12	Classification results based on data collected at the right ankle and features extracted using 10.24 second windows.	77

LIST OF FIGURES

2.1	Triaxial accelerometer data from the 400 meter walk for a single individual (top left) and a zoomed 10 second window (top right). Vector magnitude from the 400 meter walk for same individual (bottom left) and zoomed 10 second window (bottom right).	5
2.2	Pre-processing data. Observed FFT spectra for one subject as described in Step 4 of Table 2.1 (top left). Observed spectra realigned into order domain for the same subject as described in Step 6 of Table 2.1 (top right). Average realigned spectra for all subjects as described in Step 7 of Table 2.1 (bottom left). Scaled average spectra for all subjects as described in Step 9 of Table 2.1 (bottom right).	12
2.3	Pre-processed walking spectra (left) and basis functions used for modeling (right). The x-axis represents multiples of the frequency of the cadence.	16
2.4	Estimates of the coefficient function, $\tilde{\beta}$, (with 95% point-wise confidence band) for the association of walking with (a) age and (b) BMI as described in Section 2.4. The x-axis represents multiples of the frequency of the cadence.	16

3.1	Raw accelerometry data for Subject 14 during the walking trial. Each panel represents different sections of the walking trial. The top left panel contains data from the first segment of walking on level ground from the start of the trial to the first set of stairs. The top middle panel represents the first set of stairs where the participant descended the stairs, ascended the stairs, and descended the stairs again prior to proceeding into walking on the second walking section (top right panel).	24
3.2	Fourier spectrum (left) and power spectrum (right) with shaded regions describing the features derived from the FFT. In the top figure, the shaded region represents the numerator of ratio.VM , and the dominant frequency is labeled as f1 . In the bottom figure, the shaded region represents p1	29
3.3	Boxplots for sensitivity (top left), specificity (top right), PPV (bottom left), and F1 score (bottom right) across participants by activity, sensor location, and window length.	35
3.4	Variable importance rankings for the twelve scenarios. Variables are sorted from top to bottom by median importance rank.	39
4.1	Raw triaxial accelerometer data of level walking (top row), descending stairs (middle row), and ascending stairs (bottom row) for Subject 14 (left column) and Subject 20 (right column) obtained from the left wrist accelerometer.	46

4.2	Raw triaxial acceleration signal with different colors representing data from each axis (left column) and vector magnitude (right column) for 10 seconds of level walking (top row), descending stairs (middle row), and ascending stairs (bottom row) for a single subject’s data collected at the left wrist.	52
4.3	Fourier spectra (left column) and wavelet decomposition (right column) for 10 seconds of level walking (top row), descending stairs (middle row), and ascending stairs (bottom row) for a single subject’s data collected at the left wrist.	53
4.4	Fourier spectrum (left) and power spectrum (right) with shaded regions describing the features derived from the FFT. In the left figure, the shaded region represents the numerator of ratio.VM , and the dominant frequency is labeled as f1 . In the right figure, the shaded region represents p1	54
4.5	Vector magnitude for 10.24s windows of level walking (top row), descending stairs (middle row), and ascending stairs (bottom row) for Subject 14 (left column) and Subject 20 (right column).	57
4.6	Sensitivity and specificity by activity, sensor location, and window length.	61
4.7	Positive predictive value and F1 score by activity, sensor location, and window length.	62
4.8	Variable importance rankings for the twelve scenarios. Variables are sorted from top to bottom by median importance rank.	63

4.9	Final classification tree for data collected at the hip and features extracted using 2.56 second windows.	66
4.10	Final classification tree for data collected at the hip and features extracted using 5.12 second windows.	67
4.11	Final classification tree for data collected at the hip and features extracted using 10.24 second windows.	68
4.12	Final classification tree for data collected at the left wrist and features extracted using 2.56 second windows.	69
4.13	Final classification tree for data collected at the left wrist and features extracted using 5.12 second windows.	70
4.14	Final classification tree for data collected at the left wrist and features extracted using 10.24 second windows.	71
4.15	Final classification tree for data collected at the left ankle and features extracted using 2.56 second windows.	72
4.16	Final classification tree for data collected at the left ankle and features extracted using 5.12 second windows.	73
4.17	Final classification tree for data collected at the left ankle and features extracted using 10.24 second windows.	74
4.18	Final classification tree for data collected at the right ankle and features extracted using 2.56 second windows.	75
4.19	Final classification tree for data collected at the right ankle and features extracted using 5.12 second windows.	76
4.20	Final classification tree for data collected at the right ankle and features extracted using 10.24 second windows.	77

Chapter 1

Introduction

Various methods exist to measure physical activity (PA). Subjective methods, such as diaries and surveys are relatively inexpensive ways of measuring one's PA; however, they are riddled with measurement error and bias due to self-report. Wearable accelerometers offer a noninvasive and objective measure of subjects' PA and are now widely used in observational studies. Accelerometers record high frequency data and produce an unlabeled time series at the sub-second level. An important activity to identify from the raw accelerometry data is walking, since it is often the only form of exercise for certain populations. Currently, most methods use an activity summary which ignores nuances of walking data such as gait characteristics, complexity, and vector magnitude.

In their most basic form, an accelerometer is an electro-mechanical device that measures acceleration along three orthogonal axes [Urbanek et al. (2015)]. The acceleration is measured in units of gravity and sampled in a range from 30 to 100Hz. Current devices are often the size of a typical watch and can be attached to a number of locations on the human body, but most often they are attached to the wrist, hip, or ankles of participants. Many devices produce summarized activity summaries based on proprietary algorithms that vary between devices. Our interest is in developing transparent methodology for working with the raw accelerometry data that is robust to the many devices available. Specifically, this dissertation focusses on data

obtained from individuals while performing different walking tasks (i.e., walking on level ground, ascending stairs, and descending stairs).

In Chapter 2, we propose methodology to model specific health related outcomes (scalar response variable) with a functional linear model utilizing spectra obtained from the local fast Fourier transform (FFT) of walking as a predictor. Utilizing signal processing techniques, the walking spectra are transformed from the frequency domain to the order domain so the spectra across subjects are aligned. Utilizing prior knowledge of the mechanics of walking, we incorporate this as prior information about the structure of our transformed walking spectra. Methods are applied to the in-the-lab data obtained from the Developmental Epidemiologic Cohort Study (DECOS). The data were collected at the University of Pittsburgh as part of broader study of physical activity in a normal aging population.

In Chapter 3, we are interested in classifying different types of walking. More specifically, we are concerned with differentiating between walking on level ground, ascending stairs, and descending stairs. As these activities appear very similar in their raw data form, we propose to extract a set of relevant features from the raw data and investigate their predictive power in terms of subject level classification. We build our predictive models using the classification tree methodology as described by Therneau and Atkinson (2015). We evaluate the properties of the models built with data collected from four body locations (i.e., left wrist, left hip, left ankle, and right ankle) and features extracted using three window lengths (i.e., 2.56, 5.12, and 10.24 seconds). Understanding which features provide the best discrimination under a wide range of data collection scenarios is imperative to the design of successful studies.

In Chapter 4, we expand upon our work in Chapter 3 to the population level.

Due to extensive heterogeneity between subjects, we are unable to directly compare raw data and extracted features between subjects. Therefore, we propose a novel normalization of the walking data to walking on level ground. Once data are normalized, we build classification models similar to those in Chapter 3 and evaluate their performance. We also evaluate the feature importance under the population scenario in order to validate our findings in Chapter 3.

In Chapter 5, we wrap up this dissertation with a brief discussion. We will discuss the value added and limitations of the work discussed within this dissertation as well as the future research directions.

Chapter 2

Functional Linear Models to Detect Associations between Characteristics of Walking and Health Indicators using Accelerometry Data

2.1 Introduction

Wearable accelerometers have become increasingly common in studies of physical activity, aging, and obesity [Copeland and Esliger (2009); Gardner and Poehlman (1998); Lange-Maia et al. (2015); Pruitt et al. (2008); Richardson et al. (2014)]. Self-report measures such as questionnaires have been widely used to assess physical activity (PA) previously [Pruitt et al. (2008)]. However, questionnaires require individuals to recall their daily activities which can be extremely difficult, particularly for older individuals [Baranowski (1988)]. Often, memory limitations among older individuals bring a significant amount of recall bias into the measurements provided. Schrack et al. (2013) showed there are changes in the daily patterns and amount of PA as people age. To further understand the relationship between PA and age, it is informative to assess the relationship between age and characteristics of walking because short periods of walking may be the only PA achieved by many individuals in an elder population. According to the CDC, walking is the most popular form of aerobic physical activity [<https://www.cdc.gov/vitalsigns/walking/> (Accessed: 05/03/2017)]. Accelerometers offer a non-invasive and objective alternative to self-report methods. Advancements in data processing now allow for the analysis of specific gait characteristics such as cadence and asymmetry [Moe-Nilssen and Helbostad (2004)]. Likewise,

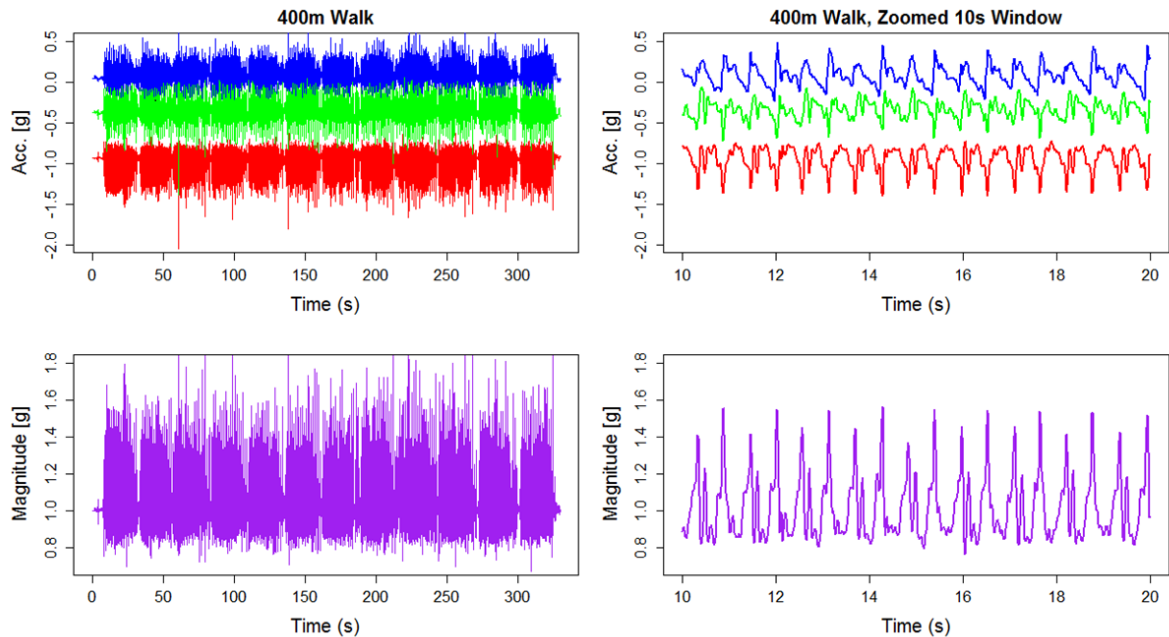


Figure 2.1: Triaxial accelerometer data from the 400 meter walk for a single individual (top left) and a zoomed 10 second window (top right). Vector magnitude from the 400 meter walk for same individual (bottom left) and zoomed 10 second window (bottom right).

advancements in statistical methodology for analysis of high dimensional data have opened up new paths for analyzing more complex, and potentially more informative, summaries of accelerometry data. In this manuscript, we propose a novel application of recently developed statistical methods to the analysis of accelerometry data by associating scalar outcomes, such as age and BMI, to the Fourier spectrum of walking.

Accelerometers are electro-mechanical devices that measure acceleration along three orthogonal axes. They are often worn on a person’s waist and provide high frequency, high-throughput data represented by three time series of acceleration measurements along three orthogonal axes [Sandroff et al. (2012); Urbanek et al. (2015)]. The data are typically collected at the sub-second level (usually between 10 to 100

observations per second), however most studies aggregate the data over one minute epochs, or windows, and often, using a user specified threshold, the data are characterized into activity counts per minute. While thresholding methods are useful in describing the timing and duration for certain levels of PA, many nuances of the data are lost. For example, it is not possible to evaluate how a person is walking from activity count summaries. Especially in an at risk population, such as elder or obese populations, this raises the question as to whether a more detailed quantification of the walking signal can provide additional information. For example, if an elder person's legs are bothering them, we may detect signs of limping that could help explain the low levels of PA.

To illustrate the complex nature of the data collected, Figure 2.1 shows the raw data collected from a triaxial accelerometer for a single individual during an in-lab 400 meter walk. The top left panel of Figure 2.1 presents the entire 400 meter walk, where each axis is shown in a different color. With just over 5 minutes worth of data, the characteristics of the signal are nearly impossible to visualize. The top right panel of Figure 2.1 shows a 10 second window of the same data. When zoomed in, we can discern a fairly periodic signal. The periodic characteristics of walking naturally lend themselves to a frequency analysis approach for quantifying the features of walking. Utilizing similar methods to those described in Urbanek et al. (2015), we can extract estimates of cadence (steps per second) and average magnitude from windows of raw data. In addition to these more common features, we also utilize the spectra obtained from the local Fast Fourier Transform (FFT) as a functional predictor for modeling the association of walking with scalar health related outcomes such as age and body mass index (BMI). By incorporating the walking spectra as a predictor, we

gain additional information about the characteristics of a person’s gait which may be associated with the outcome of interest. For example, an individual with a very smooth walking stride would result in most of the energy from walking concentrated around the frequencies near the cadence. However, an individual with an interrupted stride (e.g. a limp) would result in energy being more spread out through higher frequencies.

Several methods exist for fitting a scalar-on-regression function such as $y = \int_{\mathcal{I}} x(t)\beta(t)dt + \epsilon$, where $x(\cdot)$ is a functional predictor and y is a scalar response variable. Several methods for estimating $\beta(\cdot)$ are based on the eigenfunctions associated with some covariance operator defined by the predictors [Randolph et al. (2012)]. Ramsay and Silverman (2006) describe a number of methods that involve combinations of empirical eigenfunctions or B-splines, but fail to provide methods for incorporating prior knowledge of the structure into the estimation. Due to the periodic nature of walking, we have strong reason to believe the vast majority of information contained in the walking spectra will be located around the harmonics centered at multiples of the dominant frequency. Therefore, the method developed by Randolph et al. (2012), which allows for the incorporation of presumed structure directly into the estimation process, is preferable to a purely empirical estimator.

The remainder of this paper is structured as follows. In Section 2.2, we describe the data collection and pre-processing procedures. In Section 2.3, we describe the functional linear model used to fit the data and how estimation is performed. In Section 2.4, we apply the proposed model to data collected in the lab from a study of an elder population. In Section 2.5, we conclude with a discussion.

2.2 Data collection and pre-processing

Data were collected in the Developmental Epidemiologic Cohort Study (DECOS), a study of elderly individuals in good health. The study was conducted at the University of Pittsburgh, by Nancy Glynn, and was designed to evaluate established tools for measuring physical activity, fatigability, fitness, and muscle function as they relate to physical function with the purpose of establishing optimal tools for future epidemiologic studies in older adult populations. This paper focuses on $N = 46$ individuals who completed the “in-the-lab” fast-paced 400 meter walk [Lange-Maia et al. (2015)]. Data were collected using an Actigraph GT3X+ worn at the right hip. The raw data were sampled at 80Hz.

The first step in pre-processing the data is to split the observed triaxial signal from the 400 meter walk into 10 second non-overlapping windows. For each window, we transform the raw triaxial signal into vector magnitude (VM), where VM is defined as the root sum of squares of the three axes, i.e. $vm(t) = \sqrt{x_1(t)^2 + x_2(t)^2 + x_3(t)^2}$. The vector magnitude count (VMC) is then calculated as the mean absolute deviation of the VM ,

$$v_\tau(t) = \frac{1}{\tau} \sum_{u=t-\tau/2}^{t+\tau/2} |vm(u) - \overline{vm}|, \quad (2.1)$$

where τ is the window size expressed as number of sampling points, as defined in Urbanek et al. (2015). We then transform the VM from the time domain into the frequency domain using the local FFT, or short time Fourier transform (STFT). Similar to Urbanek et al. (2015), we define the STFT at time t of the $vm(t)$ as $X(t, f; \tau) = \sum_{u=[t-\tau/2]}^{[t+\tau/2]} vm(u)h(u)e^{-i2\pi fu/\tau}$, where τ is a tuning parameter specifying

the number of observations in the interval centered at t . The Hanning weights, defined as, $h(u; \tau) = 0.5[1 - \cos\{2\pi u/(\tau - 1)\}]$ are used to avoid a blurring of the obtained spectra.

For each spectrum obtained, we then identify the fundamental frequency (cadence) as the location of the largest peak in the spectrum. Since the usual speed of walking is between 1.4 - 2.5 Hz, as reported in Pachi and Ji (2005), we chose to look for the cadence in a conservative range of 1.2 - 4.0 Hz to be consistent with Urbanek et al. (2015). The frequency axis used is from 0Hz to 39.9Hz sampled every 0.1Hz which ensures every individual's spectra will contain at least 10 multiples of their dominant frequency, or cadence.

In order to align all spectra at their cadence, we further transform each spectrum from the frequency domain into the order domain by scaling the frequency axis by the cadence for each spectrum. Linear interpolation is used to put each spectrum back on the same sampling grid. This ensures that all spectra are aligned and sampled at equally spaced points.

Since each spectrum is sampled discretely, further harmonics may be misaligned in the order domain. To compensate, we average the spectra across all windows for each subject in order to obtain a global estimate of walking features for each individual. Each spectrum is restricted to 546 points between 0.3 and 5.75 in the order domain to avoid modeling signal noise at the beginning and end of the spectra.

Finally, we scale each individual's average spectrum by the magnitude of the spectrum at the cadence. By scaling the spectra in this way, the magnitude at each harmonic can be interpreted as a ratio to the magnitude at the cadence. This process is illustrated in Figure 2.2 and fully detailed in Table 2.1. These steps for

pre-processing the raw accelerometry data are essential in order to properly fit the statistical model described in Section 2.3.

2.3 Statistical Methods

Let $W_i(\cdot)$ denote a functional predictor from the i^{th} subject ($i = 1, \dots, N$). We will assume each observed predictor is a discretized sampling from an idealized function at p equally spaced points, s_1, \dots, s_p , as can be seen in the walking spectra in Figure 2.2. We let $w_i := [w_i(s_1), \dots, w_i(s_p)]^T$ be the $p \times 1$ vector of values sampled from $W_i(\cdot)$. Then our observed data take the form $\{y_i; x_i; w_i\}$ where y_i is a scalar response, x_i is a $K \times 1$ vector of measurements from K scalar predictors, and w_i is the functional predictor from the i^{th} subject. We denote the true coefficient function by $\beta(\cdot)$, and then, the functional regression model of interest is given by

$$y_i = x_i^T \gamma + \int_{\mathcal{I}} W_i(s) \beta(s) ds + \epsilon_i \quad (2.2)$$

where $\epsilon_i \sim N(0, \sigma_\epsilon^2)$. Here $x_i^T \gamma$ is the linear effect from K scalar predictors and $\int_{\mathcal{I}} W_i(s) \beta(s) ds$ is the functional effect.

2.3.1 Estimation of Parameters

The approach proposed in Randolph et al. (2012) assumes y_i is linearly dependent on $W_i(\cdot)$ at the p sampling points, w_i . We impose functional structure into the estimation of $\beta(\cdot)$. Then, combining all N subjects, we can express equation 2.2 as

Table 2.1: Algorithm 1

Input: $x(t)$ - accelerometry signal, f_s - sampling frequency, $s_{min} = 1.2Hz$, $s_{max} = 4.0Hz$

Output: FFT - scaled average FFT spectrum, VMC - average VMC, $Cadence$ - average cadence

Step 1. Divide accelerometry signal into 10 second non-overlapping windows.

Step 2. Transform accelerometry signal into vector magnitude $vm(t)$.

Step 3. Compute vector magnitude count, $v_{10}(t)$, for each window.

Step 4. Compute Fourier spectrum for each window.

Step 5. Estimate cadence as frequency centered under the largest peak in spectrum.

Step 6. Transform spectra from frequency domain to order domain by scaling frequency axis by the frequency of the cadence.

Step 7. Average vector magnitude count, cadence, and order domain spectra across all windows.

Step 8. Restrict spectra to points between 0.3 and 5.75 multiples of the cadence frequency.

Step 9. Scale spectra by magnitude of the average spectra at the cadence.

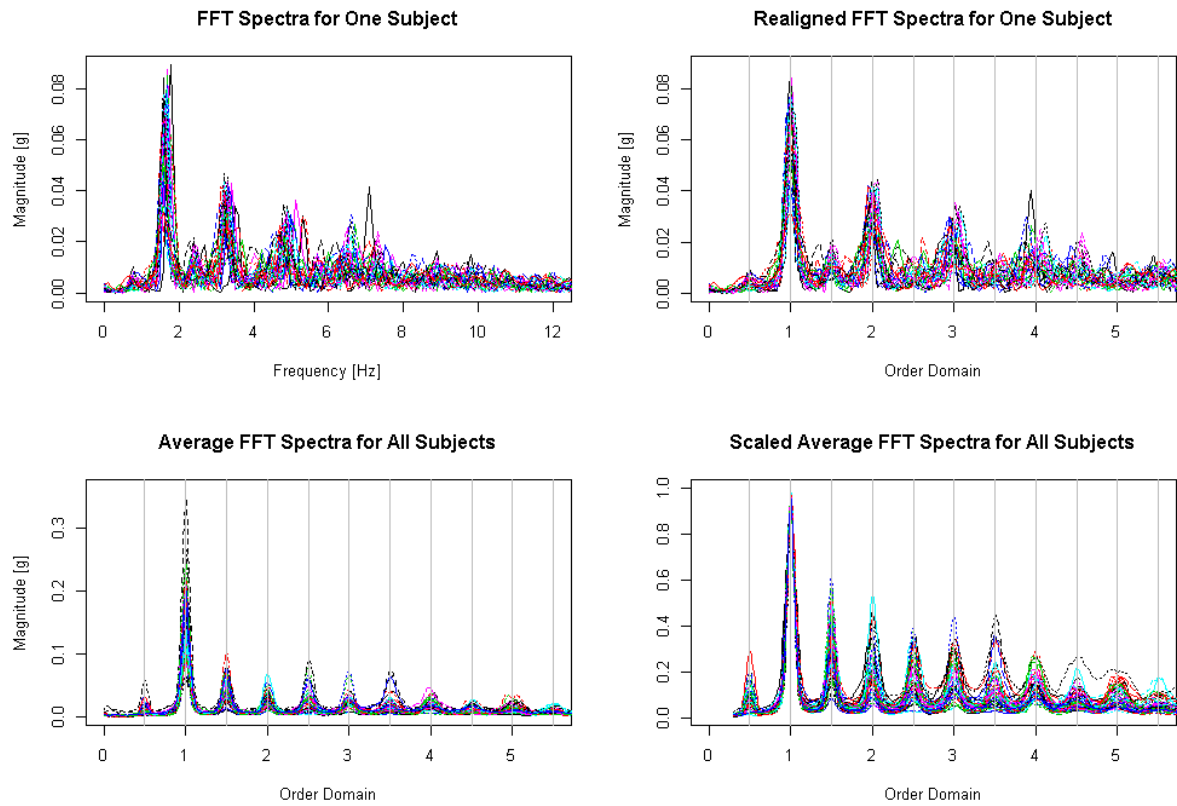


Figure 2.2: Pre-processing data. Observed FFT spectra for one subject as described in Step 4 of Table 2.1 (top left). Observed spectra realigned into order domain for the same subject as described in Step 6 of Table 2.1 (top right). Average realigned spectra for all subjects as described in Step 7 of Table 2.1 (bottom left). Scaled average spectra for all subjects as described in Step 9 of Table 2.1 (bottom right).

$$y = X\gamma + W\beta + \epsilon \quad (2.3)$$

where $y = [y_1, \dots, y_N]^T$ is an $N \times 1$ vector of responses, $X = [x_1^T, \dots, x_N^T]^T$ is an $N \times K$ design matrix corresponding to the scalar predictors with coefficient vector γ , $W = [w_1^T, \dots, w_N^T]^T$ is an $N \times p$ design matrix corresponding to the functional predictors with functional coefficient vector β .

Due to our belief that the relevant information contained in the walking spectra is localized around the harmonics at multiples of the dominant frequency, we want to estimate β while imposing some prior knowledge on its functional structure. We achieve this by incorporating an informed penalty operator, L , as proposed in Randolph et al. (2012). The penalized estimates of γ and β are obtained by

$$[\tilde{\gamma}, \tilde{\beta}_{\lambda, L}]^T = \arg \min_{\gamma, \beta} \{ \|y - X\gamma - W\beta\|^2 + \lambda \|L\beta\|_{L^2}^2 \}, \quad (2.4)$$

where we only penalize the functional coefficient vector β . Given some prior knowledge about the structure of our functional predictor, our penalty can be defined as a subspace containing this information [Randolph et al. (2012)]. We define an informative space, Q , to be a span of basis functions emphasizing the relevant features of $\beta(\cdot)$ and consider the orthogonal projection $P_Q = QQ^+$. As described in Randolph et al. (2012), we define our decomposition-based penalty as

$$L \equiv L_Q = a(I - P_Q) + P_Q \quad (2.5)$$

for some $a > 0$. Thus, when $a > 1$ the estimate is penalized more in the non-

informative space orthogonal to Q . When $a = 1$, the estimate is simply a ridge estimate. Therefore, a generalized ridge estimate of γ and β can be obtained as

$$[\tilde{\gamma}, \tilde{\beta}]^T = (X_o^T X_o + \lambda L_o^T L_o)^{-1} X_o^T y, \quad (2.6)$$

where $X_o = [X \ W]$ and $L_o = \text{blockdiag}\{0, L_Q^T L_Q\}$. The choice of tuning parameter, λ , is provided through a linear mixed model framework as described in Ruppert et al. (2003).

2.4 DECOS Example

We applied the methods discussed in section 2.3 to the data described in section 2.2 to study the association of walking spectra obtained from the fast-paced 400 meter walk with age and BMI [Lange-Maia et al. (2015)]. The fast-paced 400 meter walk is often used in epidemiological studies of older adults in order to assess aerobic fitness [Simonsick et al. (2006)]. The most common protocol implemented for the fast-paced 400 meter walk is the Long Distance Corridor Walk (LDCW) [Simonsick et al. (2001)]. The pre-processed walking spectra described in Section 2.2 were each sampled at $k = 546$ distinct sampling points within 0.3 and 5.75 of the order domain. This range was chosen because there is little energy contained in the spectra beyond 13.5 Hz. Assuming an average cadence of 2.0 Hz, this range sufficiently covers the relevant features of walking. There were $N = 46$ subjects that completed the LDCW. In addition to each subject's scaled average walking spectra, an estimate of their average cadence is used as a predictor in the proposed models to control for subject specific walking speeds. In addition, VMC was used to control for the magnitude

each subject produces. For example, an individual with a very controlled and smooth walking style will show lower magnitude than an individual with a heavy stomp in their walk. We also adjusted each model for gender differences.

In order to use our prior knowledge about the structure of the walking spectra, we define a penalty L_Q as given in equation 2.5 (with $a = 2$). We define our basis functions as normal density functions centered at multiples of the cadence from $0.5 * cadence$ to $5.5 * cadence$ using steps of 0.5. We chose a standard deviation such that the distributions were nearly orthogonal. Scaled average walking spectra and basis functions are displayed in Figure 2.3. The following model was fit to these data

$$y_i = \gamma_0 + Male_i * \gamma_1 + Cadence_i * \gamma_2 + VMC_i * \gamma_3 + \int_{\mathcal{I}} Spectrum_i(s) \beta(s) ds + \epsilon_i \quad (2.7)$$

where y_i is either age or BMI, $Male_i$ is a binary variable, $Cadence_i$ and VMC_i are the cadence and vector magnitude count for subject i , respectively. $Spectrum_i(\cdot)$ is the scaled average walking spectrum for subject i as described in section 2.2. We assume that $\epsilon_i \sim N(0, \sigma_\epsilon^2)$. We obtain the estimates as the BLUP from the mixed model formulation described in Kundu et al. (2012).

Figure 2.4 displays the estimates of $\beta(\cdot)$ along with pointwise 95% confidence bands for the two models described in equation 2.7. These figures show that the estimated regression function is different from zero at different multiples of the cadence. The regression function for age (left) shows that the coefficient function, $\tilde{\beta}$, is negative at the multiples 1.5 and 3.5 and positive at the multiples 4, 4.5, and 5. These results indicate that younger individuals have larger magnitude in the lower harmonics

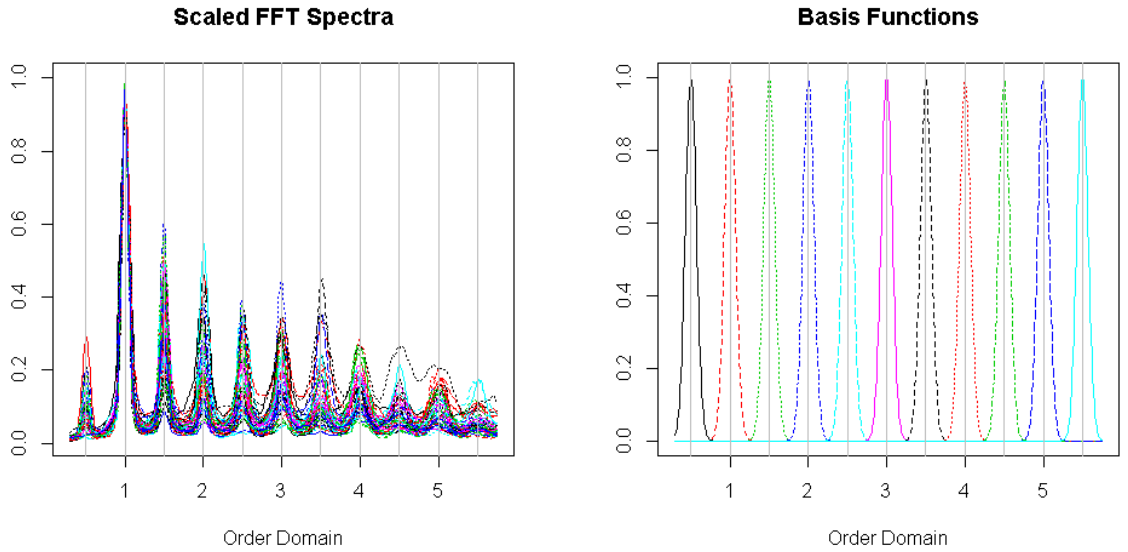


Figure 2.3: Pre-processed walking spectra (left) and basis functions used for modeling (right). The x-axis represents multiples of the frequency of the cadence.

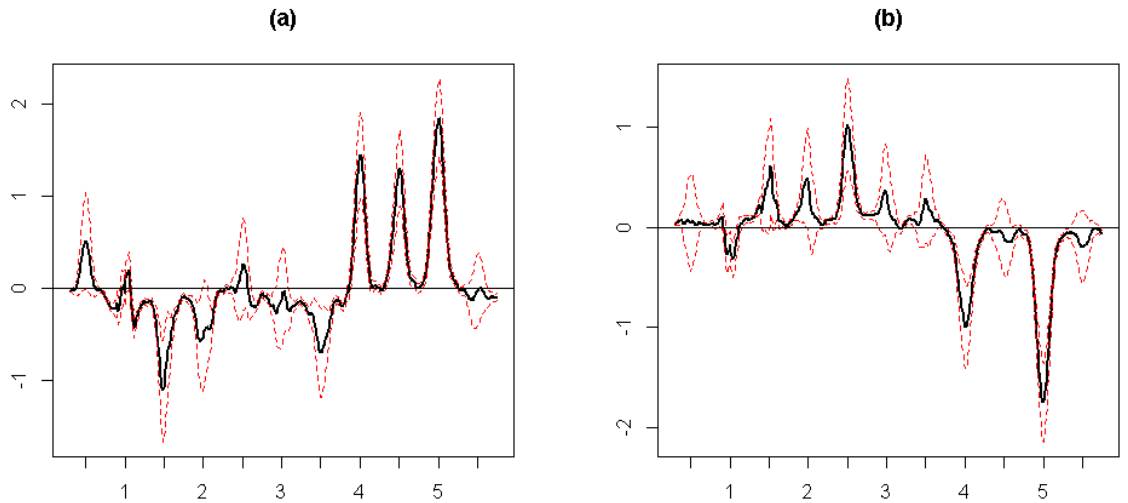


Figure 2.4: Estimates of the coefficient function, $\tilde{\beta}$, (with 95% point-wise confidence band) for the association of walking with (a) age and (b) BMI as described in Section 2.4. The x-axis represents multiples of the frequency of the cadence.

relative to the magnitude at their cadence which indicates a heavier stomp component and controlled walking motion. Older individuals have larger magnitude in the higher harmonics relative to the magnitude at their cadence which indicates a less controlled compensatory walking motion (i.e. a limp). These results are consistent with intuition and prior research [Kavanagh and Menz (2008)].

The regression function for BMI (right) shows that the coefficient function, $\tilde{\beta}$, is positive at the multiple 2.5 and negative at the multiples 4 and 5. Likewise, these results are consistent with intuition in that overweight, or obese, individuals tend to walk with a heavier stomp component which would show up as higher magnitude in the lower harmonics. Leaner individuals would walk with a lighter stomp component with more characteristics in their walking which would show up as lower magnitude in the lower harmonics sustaining consistently over the higher harmonics.

2.5 Discussion

In this paper we proposed a novel application of existing functional linear model methods to the study of physical activity data collected by accelerometers. We proposed an algorithm for pre-processing the raw data collected from accelerometers to quantify the characteristics of walking in a more detailed manner than is typically used with activity count summaries. Utilizing the periodic characteristics of walking, we were able to reduce the dimensionality of the raw data into a form that retained some details of the original signal while allowing us to use existing statistical methods for analyses. We applied these methods to the in lab data collected from a study of healthy aging within an elder population.

While FFT has been widely used for pre-processing accelerometry data, the fea-

tures extracted from such methods have been applied to the problem of classification of activity types as opposed to associating characteristics of walking to health indicators [Mannini et al. (2013); Preece et al. (2009); Urbanek et al. (2015); Zhang et al. (2012)]. To our knowledge, this is the first proposed application of functional linear regression techniques to model the association of walking spectra with health indicators. Due to the periodic characteristics of walking, the proposed method naturally lends itself to this application where we can inform the penalty operator of where the relevant information is contained in the spectra. This method is not limited to the cross-sectional setting as demonstrated in this paper, and it is easily extended to outcomes collected longitudinally [Kundu et al. (2012)]. In addition to walking speed, this more detailed quantification of walking may provide additional information as to how certain degenerative diseases (e.g. Parkinson’s disease, multiple sclerosis) affect a person’s ability to walk over the progression of disease. Reuter et al. (2011) showed that certain walking programs can actually improve gait characteristics of individuals with Parkinson’s disease over the course of a 6-month study. Gait characteristics were measured on a specialized treadmill outfitted with specialized sensors to accurately measure foot-ground contact. The application of these proposed methods could alleviate any financial restrictions of such studies to allow for much larger randomized prospective studies to determine whether these exercise therapies actually slow down the progression of Parkinson’s disease. Usefulness of such methods can only be assessed with the inclusion of accelerometers in such studies.

We acknowledge the limitations of this study. Lack of available data has restricted the analyses presented here to the known associations between age and BMI with walking. Although age and BMI are easy to measure, the strength of this study

is that it serves as a proof of concept for how researchers can utilize these walking characteristics in the presence of more relevant health related outcomes.

Chapter 3

Differentiating Between Walking and Stair Climbing Using Accelerometry Data

3.1 Introduction

The use of wearable accelerometers in public health research of physical activity (PA) has become increasingly popular. Unlike subjective methods, such as the widely used self-report questionnaires, wearable accelerometers offer a non-invasive objective measure of a person's PA. While subjective and objective methods may provide similar results with regard to qualitative findings for age and gender (e.g., males more active than females), the adherence to PA guidelines determined from accelerometers is substantially lower than from self-report [Troiano et al. (2008)]. Furthermore, detailed quantification of PA attributable to specific activities is quite challenging and remains an elusive goal of PA monitoring research [Straczkiewicz et al. (2016)]. Body acceleration is believed to be a valuable proxy for PA in the free-living environment. However, the usual method for describing PA in the free-living environment is to use activity counts and a cut-point approach which classifies intensities of PA rather than the specific activity occurring [Esliger et al. (2011); Straczkiewicz et al. (2016); Veltink et al. (1996); Zhang et al. (2012)].

While use of accelerometers to assess PA improves estimates of duration of time spent in activities of various intensities, the current methods provide biased estimates of energy expenditures (EE). Activity counts are summarized over a given window,

and then, they are compared to preset thresholds to determine whether a subject is in sedentary, light, moderate, or vigorous PA. These methods are unable to differentiate between activities that produce similar total acceleration over time but that have differing EE [Pober et al. (2006)]. For example, walking on a level surface and ascending stairs may produce similar levels of total acceleration, but the EE from ascending stairs is nearly double that of walking on a level surface [Campbell et al. (2002)]. Although these methods are primarily used to summarize the raw accelerometry data, information about the structure of the data which may be pivotal to differentiating between activities is lost [Mannini et al. (2013)]. Recent literature has attempted to address this problem using a signal processing approach. The Fast Fourier Transform (FFT) and discrete wavelet transform (DWT) have previously been used to develop more detailed feature sets for classification of different activity types [Zhang et al. (2012)]. One disadvantage of the FFT is that we lose information from the time domain. The DWT addresses this problem by providing information in both the time and frequency domains. Due to the high dimensionality of the raw accelerometry data structure, implementing a windowing approach is still an attractive option. The short-time Fourier transform (STFT) can then be implemented within a localized window recapturing the time information. However, this approach requires the choice of an appropriate window size be made Preece et al. (2009); Urbanek et al. (2015).

The windowing approach to data segmentation is common throughout the accelerometry literature. It has been demonstrated that smaller windows provide faster activity detection and computing time, but larger windows tend to perform better in the recognition of more complex activities [Banos et al. (2014)]. There are no clear cut rules when it comes to choosing window length, but it is important to consider

the application prior to making a choice as some shorter activities could be obscured by noise in larger windows and longer activities may not be fully captured in shorter windows. Banos et al. (2014) attempted to address this problem with an extensive study of the impact of window length on activity recognition. Although they conclude the window size of 1-2s provides the best trade-off between recognition speed and accuracy, their feature set consisted only of simple metrics such as mean, standard deviation, minimum, maximum, and mean crossing rate. When the interest lies in differentiation among similar activities such as walking and stair climbing, more detailed features must be implemented which require larger window sizes for higher resolution of spectral features.

In this paper, we conducted the IU Walking and Driving Study (IUWDS) to collect accelerometry data for walking, stair walking, and driving in a simulated free-living environment. The study consisted of two separate trials, a walking trial and a driving trial. Figure 3.1 displays the raw accelerometry data from a single participant during the walking trial. Each subject was asked to complete five periods of walking on level ground and six periods, each, of ascending and descending stairs. All participants were instructed to perform each task at their usual pace to simulate data collected in a free-living environment. Using the complete data from both walking and driving trials, we were able to show that we can accurately differentiate between walking activities and driving with high accuracy [Strackiewicz et al. (2016)]. Therefore, the focus of this paper is on differentiating between different types of walking. Prior to any modeling, the raw accelerometry data were extensively pre-processed. Using a windowing approach, we extract features of data from both the time and frequency domains. Most of the chosen features provide either a measure of the energy exerted

from certain activities or measures of periodicity from the signal, and half of the features were derived from the FFT and DWT. Finally, extracted features are used to build subject specific classification trees. The classification tree was chosen because it has been shown to provide good classification of PA types [Bao and Intille (2004); Ellis et al. (2016); Kwapisz et al. (2011); Zhang et al. (2012)]. Classification trees also provide an interpretable model that can be used to inform subsequent association studies of relevant features that may be used in modeling. The classification models for each subject were built under different conditions of sensor location and window length. Model evaluation was performed to assess the impact of sensor location and window length on the classification accuracy for each of the three activity types.

The rest of this paper is organized as follows. In Section 3.2.1 we describe the data collection and labelling methods for the raw accelerometry data. In Section 3.2.2 we describe the signal processing used to extract relevant features from the raw data. In Section 3.2.3 we describe the classification model and subsequent statistical models used to evaluate the properties of the classification model. In Section 3.3 we describe the results of classification and the impact of differing window sizes and sensor location. In Section 3.4 we provide a brief description of the study results and future research.

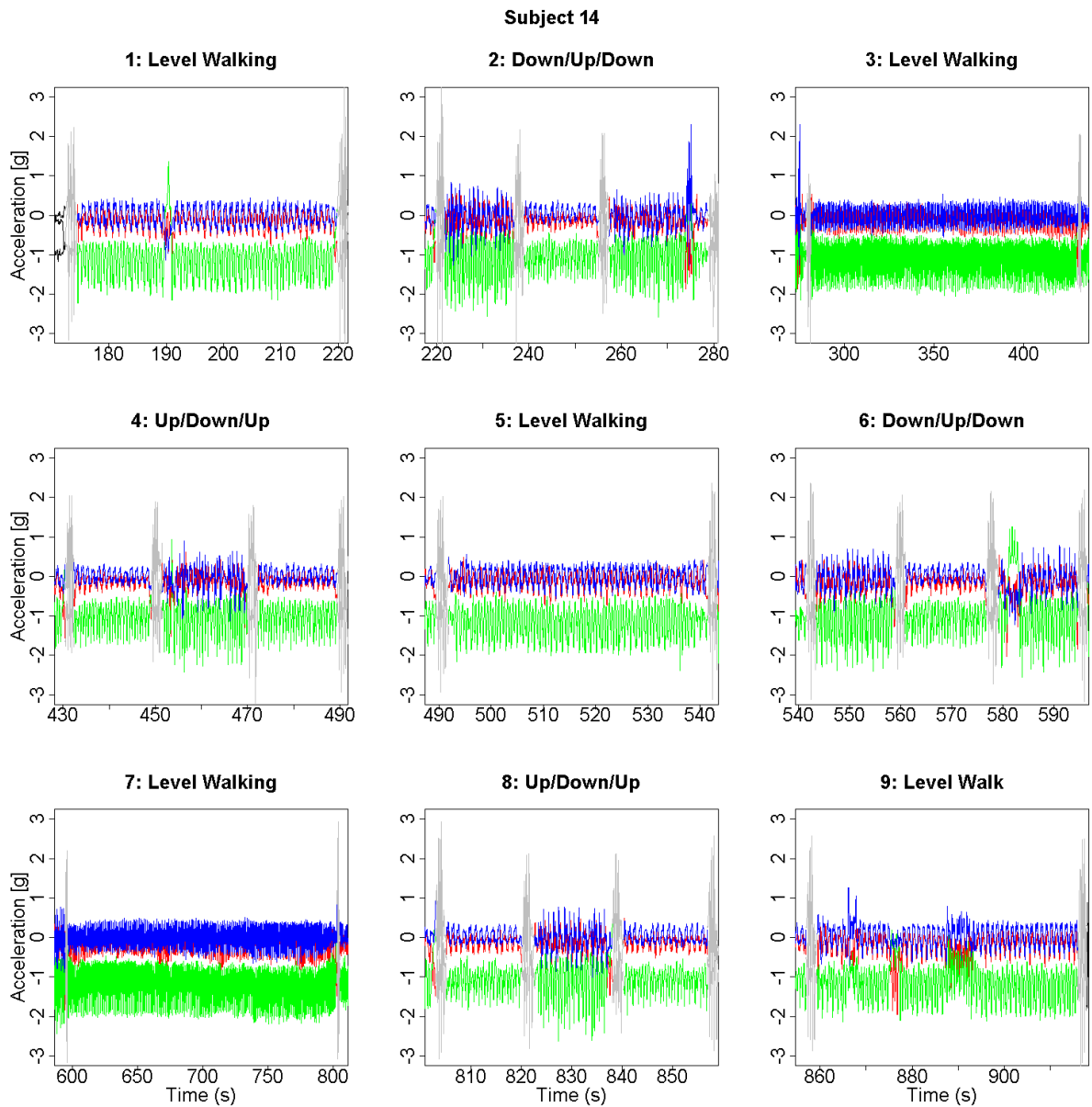


Figure 3.1: Raw accelerometry data for Subject 14 during the walking trial. Each panel represents different sections of the walking trial. The top left panel contains data from the first segment of walking on level ground from the start of the trial to the first set of stairs. The top middle panel represents the first set of stairs where the participant descended the stairs, ascended the stairs, and descended the stairs again prior to proceeding into walking on the second walking section (top right panel).

3.2 Methods

3.2.1 Data collection and labelling

Thirty-two adults (13 men, 19 women) participated in a study (IUWDS) to identify patterns of walking, stair walking, and driving from raw accelerometry data. The study was approved by the Institutional Review Board of Indiana University; all participants provided written informed consent. Participants wore four ActiGraph GT3X+ accelerometers: one on the left ankle, one on the right ankle, one on the left hip, and one on the left wrist. All four devices were synchronized to the same external clock providing parallel measurement for the four body locations. Each device was attached using velcro bands. The ankle accelerometers were worn on the outside of the ankles. The wrist accelerometer was worn similar to a watch on the top of the left wrist. The hip accelerometer was attached to the belt of the participant on the left hip, but when a belt was not available, the device was either attached to the corresponding belt loop or clipped to the waistband. Data were downloaded immediately following each participant's session. A human observer recorded the starting and stopping times for the walking study. All devices were initiated and data downloaded using the manufacturer's software (ActiLife version 6.12.0) [<http://actigraphcorp.com>]. Table 3.1 contains demographic information for the study participants. Thirty-one of the participants were right handed while the remaining individual identified as ambidextrous. The study included a walking trial (approximately 0.66 miles) followed by a driving trial (approximately 12.8 miles). The walking trial included walking on level ground, ascending stairs, and descending stairs. Immediately after the walking period, participants were accompanied to their

Table 3.1: Study Demographics

Gender	N	Statistic	Mean	St. Dev.	Min	Max
Female	19	Age (y)	39.3	8.9	24.0	54.0
		Height(in)	65.8	3.7	58.0	73.0
		Weight(lbs)	143.0	32.1	100.0	212.0
		BMI (kg/m ²)	23.2	4.9	17.7	33.3
		Walk Time (mm:ss)	11:36	01:11	09:01	13:49
Male	13	Age (y)	38.6	9.5	23.0	52.0
		Height(in)	72.0	2.0	70.0	76.0
		Weight(lbs)	208.7	47.3	140.0	310.0
		BMI (kg/m ²)	28.2	5.5	20.1	39.8
		Walk Time (mm:ss)	11:31	00:58	09:47	13:01

vehicle, which they drove on a predefined route that included both highway and city driving. The walking trial lasted between 9.0 and 13.5 minutes while the driving trial lasted between 18 and 30 minutes, depending on traffic.

The data collection protocol requested participants to walk at their usual pace along a predefined course to simulate free-living activities. Our prior experience has demonstrated the inaccuracy of human observers labelling activities. In order to ensure accuracy of the starting and stopping times for different activities, participants were asked to clap three times at the beginning and end of each activity internally marking the raw accelerometry data for the wrist with three consecutive spikes in the signal. Using these internal markings within the data, we were able to accurately assign activity labels for each section of the protocol. Once activity labels were assigned, the clapping signal ± 0.5 second of data were deleted to mimic smooth transitions between activities. The walking trial consisted of five periods of walking

on level ground, six periods of descending stairs, and six periods of ascending stairs. The data from one participant include an additional period of walking on level ground due to the participant briefly forgetting the directions before turning around to ascend the stairs. For the purposes of this paper, we focus strictly on data from the walking trial collected at the four sensor locations.

3.2.2 Signal processing and feature extraction

For each participant, we assume that we can identify periods of walking by utilizing the algorithm developed by Urbanek et al. (2015) so we select only the walking trial data. Their method uses a frequency analysis approach to detect periodic activity within windowed portions of the raw triaxial accelerometry signal. They compute a signal to noise ratio from the frequency spectrum obtained by FFT that indicates periodic activity when this ratio exceeds a pre-specified threshold. This ratio (*ratio.VM*) is described in more detail below.

We consider the triaxial signal $\mathbf{x}(t) = \{x(t), y(t), z(t)\}$ where $x(t)$, $y(t)$, and $z(t)$ are the measurements along the three orthogonal axes of the device at time t . Participants walking while swinging their arm change the orientation of the wrist worn device with respect to earth’s gravity which directly affects the measurement in each axis [Bai et al. (2012); He et al. (2014); Straczekiewicz et al. (2016); Xiao et al. (2016)]. In order to remove the effects of sensor orientation, we consider the vector magnitude, *VM*, defined as:

$$VM(t) = \sqrt{x(t)^2 + y(t)^2 + z(t)^2} \tag{3.1}$$

For feature extraction, we then divide the signal into windows of 2.56, 5.12, and 10.24 seconds providing 256, 512, and 1024 samples per window (i.e. $2.56s \times 100Hz = 256$ samples), respectively. We use a set of windows of varying lengths in order to evaluate the impact of window size on feature importance and classification accuracy. Window sizes were chosen to ensure the number of samples in each window was a power of 2 to simplify computation of FFT and DWT and avoid the need for zero-padding. In addition, the smallest window of 2.56s ensures that a gait cycle is repeated at least twice. The number of windows analyzed varies by subject due to variability in the lengths of time to complete the walking trial. Similar to Zhang et al. (2012), we extract features in both the frequency and time domains. The frequency domain features are derived from the FFT and the DWT of the *VM*.

Sejdić et al. (2009) and Strackiewicz et al. (2016) refer to the sliding window FFT as the short-time Fourier Transform (STFT). For a window of size τ , centered at time t , the STFT of the signal $x(t)$ is defined as

$$X(f, t) = \sum_{u=[t-\tau/2]}^{[t+\tau/2]} x(u)h(u)e^{-i2\pi fu/\tau} \quad (3.2)$$

where f is the frequency index and the weights $h(u)$ assign more weight to observations close to t . We use the weights defined by the Hanning window, $h(u; \tau) = 0.5[1 - \cos\{2\pi u/(\tau - 1)\}]$, as they have been shown to reduce aliasing, or blurring of the spectrum [Harris (1978); Urbanek et al. (2015)]. The features extracted from the frequency spectrum of each window include:

- $f1$ - where $f1$ is the dominant frequency between 1.2-4.0 Hz and provides an estimate of the cadence (steps/second)

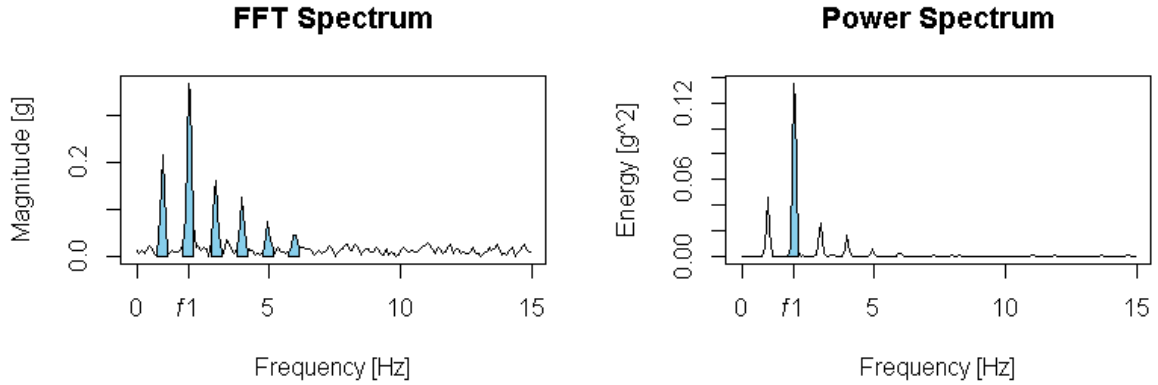


Figure 3.2: Fourier spectrum (left) and power spectrum (right) with shaded regions describing the features derived from the FFT. In the top figure, the shaded region represents the numerator of **ratio.VM**, and the dominant frequency is labeled as **f1**. In the bottom figure, the shaded region represents **p1**.

- *ratio.VM* - ratio of the partial area under the spectrum to total area under the spectrum defined in Strackiewicz et al. (2016); Urbanek et al. (2015)
- *p1* - partial area under the power spectrum at *f1*
- *p1.TP* - ratio of *p1* to the total area under the power spectrum between 0.3-12.5 Hz

Figure 3.2 provides a visual description of the features extracted from the FFT. While *ratio.VM* and *p1.TP* appear similar in concept, *p1.TP* contrasts the power of each step versus the entire spectrum, while *ratio.VM* contrasts multiple characteristics of walking versus the non-walking related portions of the spectrum. In essence, if we consider all relevant human movement to occur between 0.3-12.5 Hz, *p1.TP* is measuring the energy associated with the step component of walking versus all other movements within a given window. In contrast, *ratio.VM* is essentially measuring the periodic content of the accelerometry signal relative to the total variation associated with the *VM* signal.

Additionally, we included two DWT features similar to Zhang et al. (2012). The DWT of a signal $x(t)$ is defined as

$$x(n) = \sum_{j=1}^J \sum_{k \in Z} d_j(k) \psi^*(n - 2^j k) + \sum_{k \in Z} a_j(k) \phi(n - 2^j k) \quad (3.3)$$

where $j \in Z$ and $k \in Z$ represent the resolution, J is the depth of level, ψ is the reconstruction wavelet function and ϕ is the scaling function [Sekine et al. (2000)]. The wavelet coefficients d_j represent the details of the original signal at different levels of the decomposition, and the a_j represent the approximation of the original signal. The wavelet coefficient d_j and scaling coefficient a_j are given by

$$a_j(n) = \sum_k g(k - 2^j n) a_{j-1}(k) \quad (3.4)$$

$$d_j(n) = \sum_k h(k - 2^j n) a_{j-1}(k) \quad (3.5)$$

where g and h represent coefficients of the low-pass and high-pass filters, respectively. The features extracted from the DWT of each window are given by the following equations:

$$DWT_VM2 = \sum_{j=\alpha}^{\beta} d_j^2 / VM^2 \quad (3.6)$$

$$DWT_TP = \sum_{j=\alpha}^{\beta} d_j^2 / \sum_{j=1}^J d_j^2 \quad (3.7)$$

where $d_j^2 = d_j^T d_j$ is the sum of squared DWT coefficient vector of VM at level j ($j = 1, \dots, J$). In addition, VM^2 is the sum of the squared VM signal in each

window. For our purposes, we selected α and β to cover the frequency range 0.78-6.25Hz, and J was selected to cover the frequency range 0-12.5Hz. DWT_VM2 is the ratio of energy related to walking versus the total energy of the accelerometry signal. DWT_TP is the ratio of energy related to walking versus the total energy related to human movement. When the noise in the signal is negligible, DWT_VM2 and DWT_TP are nearly identical.

In addition to the FFT and DWT features, we also included vector magnitude count which Urbanek et al. (2015) and Straczekiewicz et al. (2016) defined as

$$VMC(t) = 1/\tau \sum_{u=[t-\tau/2]}^{[t+\tau/2]} |vm(u) - 1/\tau \sum_{u=1}^{\tau} vm(u)| \quad (3.8)$$

where $VMC(t)$ is the VMC for the window of length τ centered at t and four features derived from the raw triaxial signal: activity intensity ($ActInt = (s_x + s_y + s_z)/3$), $CORR.XY$, $CORR.XZ$, and $CORR.YZ$. We define $CORR.XY$ as

$$CORR.XY = \frac{1}{n-1} \sum_{i=1}^n \left(\frac{x_i - \bar{x}}{s_x} \right) \left(\frac{y_i - \bar{y}}{s_y} \right), \quad (3.9)$$

the Pearson correlation coefficient between the x and y axes where \bar{x} , s_x , \bar{y} , and s_y are the sample means and standard deviations of the x and y axes, respectively. $CORR.XZ$ and $CORR.YZ$ are defined similarly. The mean and standard deviation of the VM were included as the final two time domain features and defined as

$$Mean.VM(t) = \frac{1}{\tau} \sum_{u=[t-\tau/2]}^{[t+\tau/2]} vm(u) \quad (3.10)$$

and

$$SD.VM(t) = \sqrt{\frac{1}{\tau - 1} \sum_{u=[t-\tau/2]}^{[t+\tau/2]} [vm(u) - Mean.VM]^2} \quad (3.11)$$

3.2.3 Modeling

All data management and modeling was performed using RStudio version 0.99.467 [RStudio Team (2015)]. Zhang et al. (2012) showed that many machine learning algorithms provide satisfactory classification results, but the classification trees and support vector machine provide the best results. We chose classification trees for modeling the three types of walking activities due to their interpretability and ability to handle correlated predictors. We are interested in an interpretable model so that we can further understand what features are important for differentiating between the three activities. This understanding of important features will help to inform subsequent statistical analyses of walking features with relation to health related outcomes. The classification tree methodology from the R package **rpart** [Therneau and Atkinson (2015); Therneau et al. (2015)] was used for the training and testing of our classification models. We built a classification tree for each subject’s data under the 12 combinations of window length (2.56, 5.12, and 10.24 seconds) and sensor location (left hip, left wrist, left ankle, and right ankle).

In order to evaluate the performance of each classifier, cross-validation (CV) was implemented to investigate the classification accuracy of each model. To avoid over-training the classifier to identify a single activity (in our case, walking), we identified the activity (ascending or descending stairs) with the fewest windows and 60% of that sample size, n_{min} , was chosen for training from the 3 activities. We then sampled n_{min} windows of each activity for training the classifier. All remaining windows were

used for testing. This process was repeated 100 times for each participant, and the confusion matrix from the CV was used to evaluate the performance of each model. A final tree was fit for each participant using all their walking trial data using a uniform class prior to address the imbalance in the three activities.

The accuracy of each classification model was evaluated using the following metrics.

- *Sensitivity = Recall = True Positive Rate (TPR)* = $\frac{TP}{TP+FN}$
- *Specificity = True Negative Rate (TNR)* = $\frac{TN}{TN+FP}$
- *Positive Predictive Value (PPV) = Precision* = $\frac{TP}{TP+FP}$
- *F1 score* = $\frac{2*PPV*Sensitivity}{PPV + Sensitivity}$

True positives (TP) are defined as the number of windows in a given class that are correctly classified (e.g. classifying walking as walking). False positives (FP) are defined as the number of windows classified to a given class, but they actually belong to a different class (e.g. classifying walking as descending stairs). True negatives (TN) are defined as the number of windows from a given class that are not classified as a different class (e.g. classifying walking as ascending and descending stairs that are not classified as walking). False negatives (FN) are defined as the number of windows in a given class that are classified to as something else (e.g. the number of windows of walking that are classified to ascending or descending stairs). In addition to classification accuracy, we evaluated the feature set to identify which predictors provided the best separation of the three walking activities. At each iteration, a ranking of variable importance was obtained and averaged across the 100 iterations per subject. The rankings range from 1 to 13, where 1 is the most important predictor and 13 is the least important.

Linear mixed models (LMM) were used to model the effects of window size and sensor location on the classification accuracy for the three activities. Least square means were evaluated for multiple comparisons using a Tukey adjusted p-value.

3.3 Results

We applied the classification trees described in Section 3.2.3 to the walking trial data for the 32 participants in the IUWDS. As described in Section 3.2.1, data were collected from sensors placed at the hip, left wrist, left ankle, and right ankle. Participants were instructed to walk at their usual pace along a predefined course that included walking on level ground, ascending stairs, and descending stairs. The clapping periods used to internally mark the beginning and end of each activity type were removed from the raw signal in order to mimic smooth transitions between activities. Prior to modeling, the raw data were preprocessed using the methods described in Section 3.2.2. Twelve classification trees were built for each participant using the data collected from the 4 sensor locations and 3 window sizes (2.56s, 5.12s, and 10.24s). Training and testing data for each participant were constructed using the CV method described in Section 3.2.3. We evaluate each classifier in terms of sensitivity, specificity, PPV, and F1 score. Feature evaluation was performed to assess the average importance ranking of each feature included in the model. Results are presented as boxplots of the CV results, and the effects of window size and sensor location on sensitivity are investigated using LMMs.

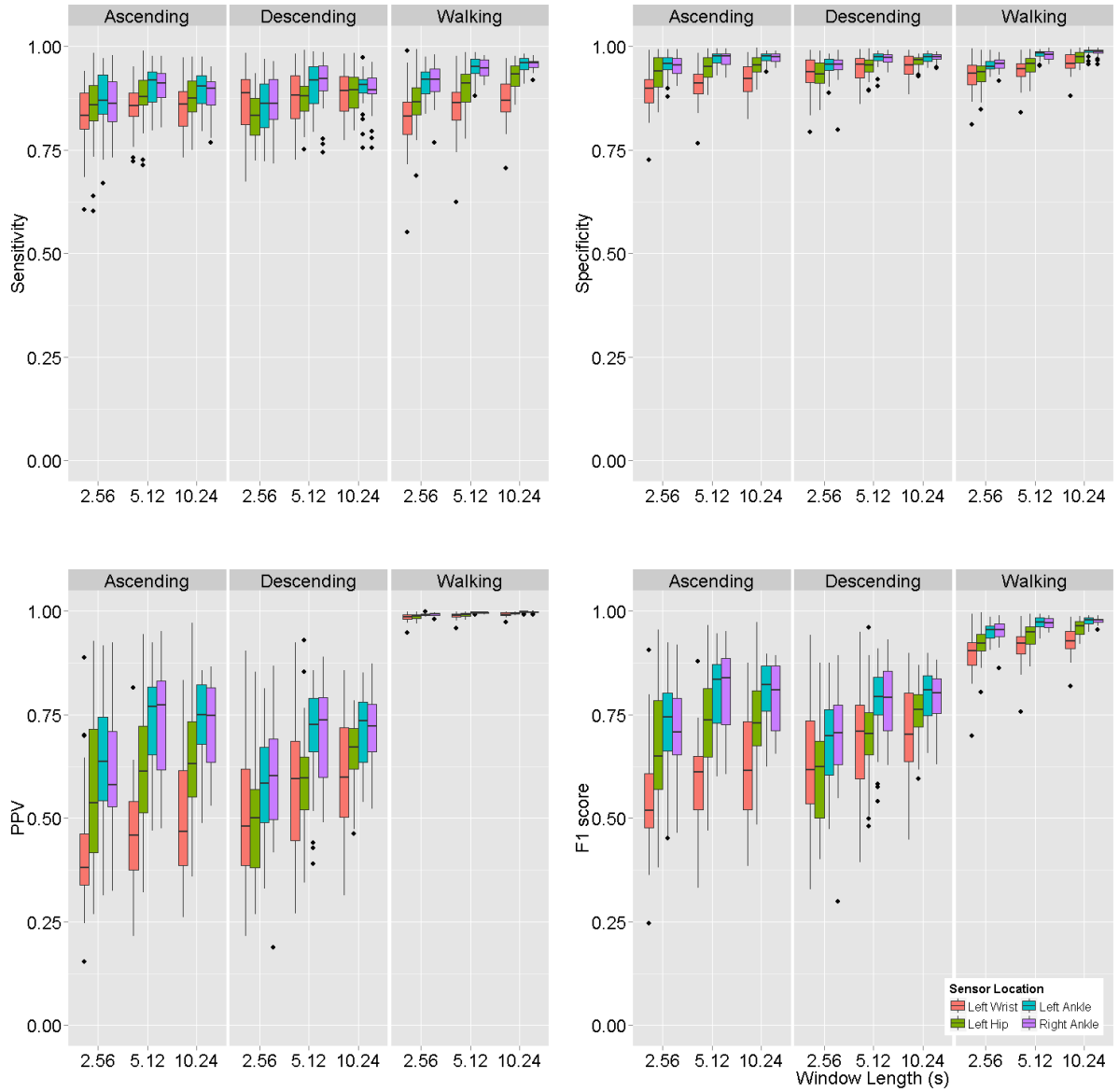


Figure 3.3: Boxplots for sensitivity (top left), specificity (top right), PPV (bottom left), and F1 score (bottom right) across participants by activity, sensor location, and window length.

3.3.1 Model evaluation

Figure 3.3 shows the results of the activity classification problem in terms of boxplots for the sensitivity, specificity, PPV and F1 score for all participants obtained from models built under each of the 12 window length and sensor location scenarios. The general trend we observe is that shorter window lengths and data collected at the wrist yield the lowest classification accuracy while larger windows and data collected at the ankles yield the highest classification accuracy. However, it appears from the top left panel of Figure 3.3 that there are differences in these trends for descending stairs. For descending stairs, the levels of sensitivity seem to be constant across window sizes for data collected from the left wrist and outperform the data collected from the hip. For the shorter window lengths (2.56 and 5.12 seconds), the sensitivity for the data collected from the wrist is higher than for the data collected at the hip.

Table 3.2: LS means of sensitivity for sensor location by activity.

Sensor Location	Activity	Mean	Lower CL	Upper CL	Group ¹
Left Wrist	Ascending	0.844	0.829	0.858	1
Left Wrist	Walking	0.852	0.837	0.866	12
Left Hip	Descending	0.863	0.849	0.877	123
Left Hip	Ascending	0.869	0.855	0.883	234
Left Wrist	Descending	0.874	0.859	0.888	234
Right Ankle	Ascending	0.885	0.870	0.899	345
Left Ankle	Descending	0.888	0.874	0.903	45
Left Ankle	Ascending	0.889	0.875	0.904	45
Right Ankle	Descending	0.889	0.875	0.904	45
Left Hip	Walking	0.900	0.885	0.914	5
Left Ankle	Walking	0.938	0.924	0.953	6
Right Ankle	Walking	0.939	0.925	0.954	6

¹ Groups with similar numbers are not significantly different from each other.

Table 3.3: LS means of sensitivity for window length by activity.

Window Length	Activity	Mean	Lower CL	Upper CL	Group
2.56s	Ascending	0.855	0.841	0.868	1
2.56s	Descending	0.855	0.842	0.869	1
10.24s	Ascending	0.876	0.862	0.889	2
2.56s	Walking	0.879	0.865	0.892	2
5.12s	Ascending	0.885	0.871	0.898	2
5.12s	Descending	0.889	0.876	0.903	2
10.24s	Descending	0.891	0.878	0.905	2
5.12s	Walking	0.914	0.901	0.927	3
10.24s	Walking	0.929	0.916	0.942	3

Table 3.4: LS means of sensitivity for sensor location.

Sensor Location	Mean	Lower CL	Upper CL	Group
Left Wrist	0.856	0.845	0.868	1
Left Hip	0.877	0.865	0.889	2
Right Ankle	0.904	0.893	0.916	3
Left Ankle	0.905	0.894	0.917	3

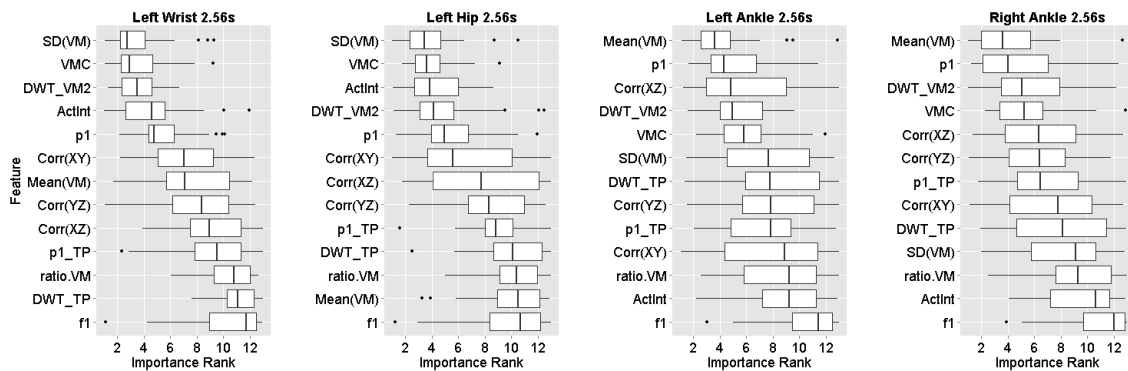
Table 3.5: LS means of sensitivity for window length.

Window Length	Mean	Lower CL	Upper CL	Group
2.56s	0.863	0.852	0.874	1
5.12s	0.896	0.885	0.907	2
10.24s	0.899	0.887	0.910	2

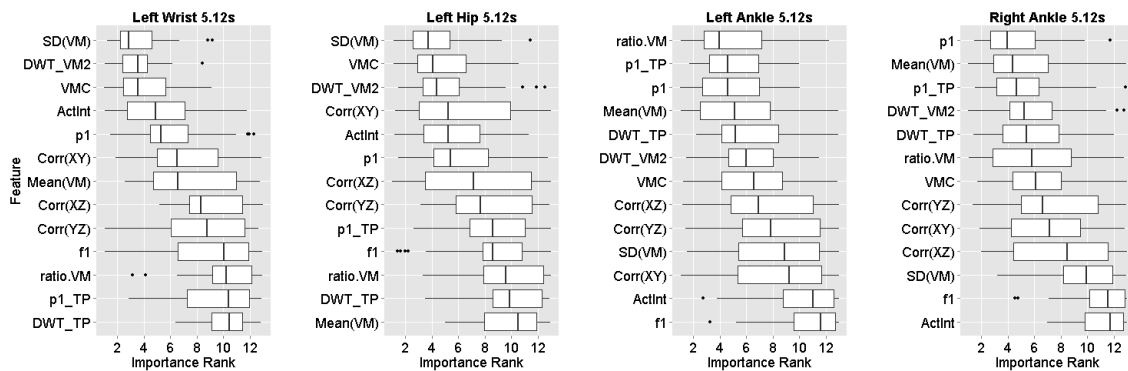
In order to investigate this interaction, we investigated the potential 3-way interaction of activity type, sensor location, and window length using a LMM. While the 3-way interaction was not statistically significant, there were significant interactions between sensor location and window length with activity type. Since these interactions were found to be statistically significant ($p < 0.001$ and $p = 0.017$, respectively), it would be inappropriate to discuss the main effects of sensor location and window length with respect to sensitivity. Tables 3.2 and 3.3 give the multiple comparison results for the sensitivity LMM of the 2-way interactions of sensor location and window length by activity type, respectively. With the exception of the sensitivity for walking and hip data, there is near perfect separation between data collected at the ankles with the hip and wrist data. Tables 3.4 and 3.5 give the multiple comparison results for the overall classification accuracy. We can see that overall, classification accuracy is the lowest with the wrist data (95% CI: 85-87%). The classification accuracy of the hip data is slightly better (95% CI: 87-89%), and the accuracy is highest among data collected at the ankles (95% CI: 89-92%, for both right and left ankles). Intuitively, the classification accuracy is lowest under the 2.56s windows (95% CI: 85-87%), and indistinguishable between the 5.12s and 10.24s windows (95% CI: 89-91%, for both).

3.3.2 Feature evaluation

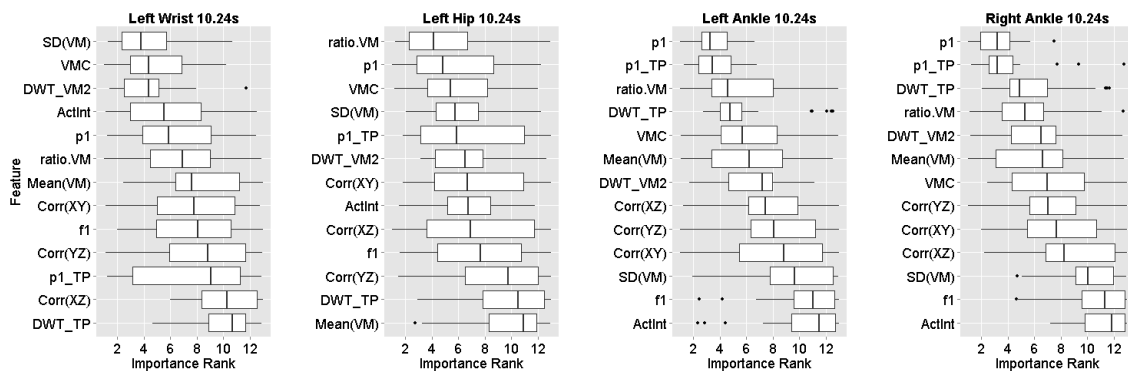
Figure 3.4 shows the distributions of the variable importance rankings for the classifiers with differing window lengths and sensor locations. For features extracted from the wrist data, we see that consistently, across all window sizes, the top five important features are $SD(VM)$, VMC , DWT_{VM} , $ActInt$, and $p1$ implying features that measure changes in the intensity of the acceleration are best at differentiating between



(a)



(b)



(c)

Figure 3.4: Variable importance rankings for the twelve scenarios. Variables are sorted from top to bottom by median importance rank.

types of walking from wrist worn devices. The same five features are also ranked most important for the hip data with 2.56s windows. The hip data with 5.12s windows includes those same features in the top six important features but also include $Corr(XY)$ with a large amount of variability in importance between subjects. When data is collected at the hip and 10.24s windows are used, the most important feature becomes $ratio.VM$ implying improved resolution of the FFT spectrum improves classification. The top two features most important for both the left and right ankle data with 2.56s windows are $Mean(VM)$ and $p1$. Consistently, $p1$ and $p1.TP$ appear in the top three most important features for the ankle data with 5.12s and 10.24s windows which implies the amplitude of $f1$ plays a significant role in differentiating between types of walking when data are collected from the ankle.

3.4 Discussion

The main objective of this study was to design algorithms for differentiating between walking on level surface, ascending stairs, and descending stairs. We evaluated the impact of sensor location and window size on the observed classification rates. The results show that the algorithms developed can classify different types of walking with good accuracy regardless of the sensor location and window size used. In addition, feature importance was compared for four sensor locations (left wrist, left hip, left ankle, and right ankle) as well as three window sizes (2.56s, 5.12s, and 10.24s). In general, ankle mounted sensors and larger window sizes showed the best classification rates. However, similar classification rates were achieved using both 5.12s and 10.24s windows. The largest discrepancies in classification accuracy was seen between different sensor locations. Wrist worn sensors yielded the lowest classification accuracy,

followed by the hip worn sensors, and then both ankle worn sensors. There were no significant differences in classification accuracy between the left and right ankles. The hip and wrist data also had much larger variability as shown in Figure 3.3.

This work extends the current literature in that we have shown that walking on level ground and stairs can be differentiated with good accuracy using relatively simple feature extraction. Improved classification of types of walking can improve estimates of energy expenditure in large scale studies. It has been shown that the relative metabolic rate while ascending a flight of stairs can be more than double that of walking on level ground, but the acceleration achieved is very similar [Ohtaki et al. (2005)]. Therefore, improved classification of types of activity above and beyond count-based thresholds may have a significant impact on how we measure PA in the future. We have also shown that feature selection is not an arbitrary choice. One must take into consideration the sensor location used in a study as well as the window size. As demonstrated in Figure 3.4, the features that are important for classification of walking and stair climbing can vary depending on where the data is collected and the choice of windowing. Our results suggest that windows smaller than 5s may have a dramatic affect on the classification accuracy achieved by any classification algorithm. In addition, the highest classification accuracy was achieved by ankle-worn sensors, but in practice, compliance with wearing a monitor on the ankle for several days is likely to be low. Although the wrist-worn device yields the lowest overall classification accuracy, it is reasonable to assume they would yield the highest rate of compliance in larger and longer studies.

The next steps in our research will be to extend the work of this paper to the population level. To achieve this, some normalization scheme must be chosen to

allow the comparison of features between subjects.

3.5 Acknowledgements

This paper was made possible, in part, with support from the Indiana Clinical and Translational Sciences Institute Design and Biostatistics Pilot Grant funded, in part by Grant UL1TR001108, from the National Institutes of Health, National Center for Advancing Translational Sciences, Clinical and Translational Sciences Award. J Harezlak has received funding from the National Institute of Mental Health research grant R01MH108467.

Chapter 4

Population Level Classification of Walking and Stair Climbing Using Accelerometry Data

4.1 Introduction

Wearable accelerometers have been increasingly used in public health studies of physical activity (PA) and clinical trials [Bussmann et al. (2001); Ermes et al. (2008); Grant et al. (2006); Hecht et al. (2009); Parkka et al. (2006); Pruitt et al. (2008); Schrack et al. (2013); Troiano et al. (2008); Welk et al. (2000)]. In contrast to self-report questionnaires, they provide an objective record of human movement at the sub-second level. The recent progress in sensor technology and wearable computing devices have allowed researchers to collect real-time information on movement through the use of accelerometers [Bai et al. (2012)]. However, identifying specific types of activity remains a challenge with accelerometry data collected in a free-living environment. Recent work done by Bai et al. (2012) and Xiao et al. (2016) has shown promise in the PA prediction field by use of dictionary of movements representing short activities which they term "movelets". However, their research was focussed on an aging population and did not address the differentiation of similar activities such as walking on level ground and climbing stairs. In this paper, we are concerned with differentiating between different types of walking (e.g., walking on level ground, ascending stairs, and descending stairs) at the population level since these activities produce similar results in terms of acceleration, but have differing levels of energy expenditure (EE).

In fact, the relative metabolic rate of ascending stairs can be nearly five times that of walking on level ground depending on the speed of walking [Ohtaki et al. (2005)]. Therefore, even short bouts of stair climbing can be an important distinction when considering an individuals overall EE throughout a given day.

4.1.1 Data

The data were collected from thirty-two adults (13 men, 19 women) that participated in a study to identify patterns of walking, stair walking, and driving from raw accelerometry data. The study included a walking trial where participants were asked to walk along a predefined course that included walking on a level ground, descending stairs, and ascending stairs. Following the walking trial, subjects who consented to the driving trial were escorted to their vehicles and asked to drive along a predefined route for approximately 30 minutes. Each participant wore four Actigraph GT3X+ accelerometers placed on the left ankle, right ankle, left hip, and left wrist. Each device was initiated to the same external computer clock providing parallel measurements for the four body locations. The sensors were attached using velcro straps. Each ankle device was attached to the outside of the ankle. The hip device was worn on the waist line attached to a belt when available or attached to the waist line of the participant's pants. The wrist worn monitor was affixed to the top of the wrist like a person would wear a watch. The raw accelerometry data was downloaded immediately following each participant's session. All data were collected at 100 Hz and devices were initialized and data downloaded using the manufacturer's software (ActiLife version 6.12.0) [<http://actigraphcorp.com>]. All participants provided written informed consent and the study was approved by the Institutional Review Board of

Indiana University.

In order to accurately identify transitions from different walking types (level walking, ascending stairs, and descending stairs), participants were asked to clap three times during each transition. This imposed internal markings of three consecutive spikes in the raw data that were then used for accurately labelling the activities. To ensure that no external noise remained in the raw data, the clapping period ± 0.5 seconds was deleted from the signal to mimic participants natural transitions between activities. The designed walking course included five periods of walking on level ground, six periods of descending stairs, and six periods of ascending stairs. One participant briefly forgot the instructions and had one additional short period of walking on level ground. Similar to our previous work in Chapter 3, we will focus solely on the data from the walking trial for this paper.

Figure 4.1 displays the raw accelerometry data obtained from the left wrist accelerometers of two subjects. In Chapter 3, we emphasized the cyclical nature of walking and climbing stairs. It should come as no surprise that the data from different subjects look similar in those respects. However, it is important to note the differences in the magnitudes of the acceleration between subject for the same activities. Because of these differences, the features extracted from the raw data may not be directly comparable across subjects. An important observation from Figure 4.1 is that these plots seem to suggest there is a consistent relationship within subjects between the different types of walking. Notice that the magnitude for walking seems to be lower than descending stairs but higher than ascending stairs. If you consider the fact that the accelerometer is measuring acceleration with respect to gravity, this should come as no surprise. When we descend stairs, we are working with gravity,

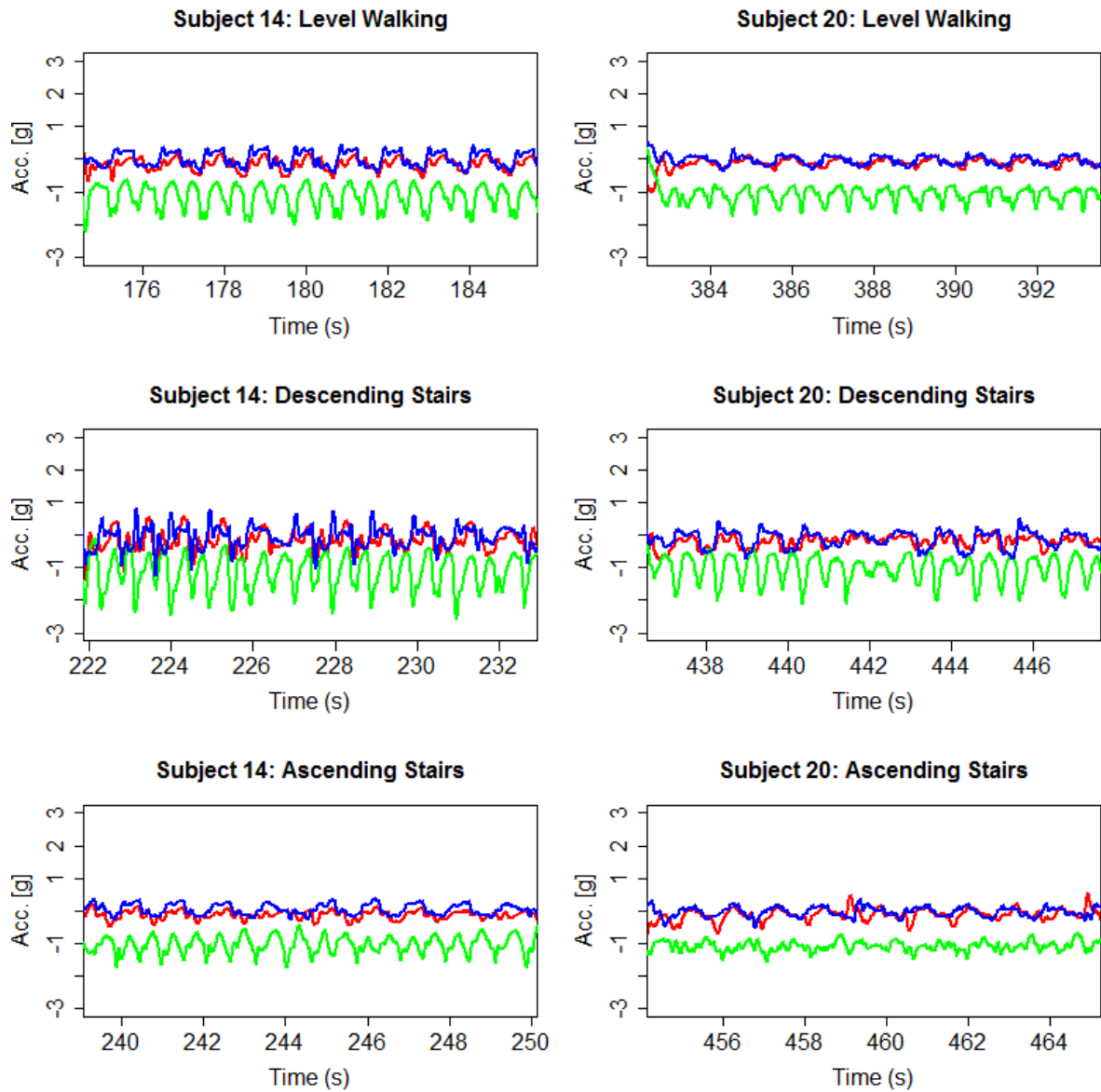


Figure 4.1: Raw triaxial accelerometer data of level walking (top row), descending stairs (middle row), and ascending stairs (bottom row) for Subject 14 (left column) and Subject 20 (right column) obtained from the left wrist accelerometer.

and when we ascend stairs we are working against gravity. It is this relationship that will guide our proposed normalization scheme.

4.1.2 Proposed methods

In this paper, we address the subject to subject variability in the magnitude of the raw accelerometry data, and thus, extracted features. We show that from using the relationship between walking and stair climbing, we can provide a robust, yet simple, transformation of the extracted features that normalizes all activities to walking. Once the data are normalized to walking, we proceed to build classification trees as we did in Chapter 3. However, to build a population level classification model, we train the classifier on a subset of subjects and test the model on the remaining subjects as opposed to sampling within subjects. This will allow us to ascertain the generalizability of our results. We will assess the accuracy of the proposed models and evaluate the predictive power of each feature included in the models. We will show that the choice of window length and sensor location have a direct impact on the features needed for classification and the accuracy of the models.

Specifically, we will use the classification tree methodology implemented in the R package **rpart** [Therneau and Atkinson (2015); Therneau et al. (2015)]. In general, the procedure looks for the feature that best splits the data into two homogeneous groups. Then the procedure is repeated on each subgroup until a stopping point has been reached in which no more improvements can be made or a minimum size has been reached for the subgroups, or nodes. In order to avoid over-fitting the model to the training data, a second step is applied to prune the tree back to a smaller size using cross-validation. We use the Gini index as a measure of impurity in the nodes

to build our tree. The result is an interpretable model that can be used to predict types of walking in a general adult population.

4.1.3 Literature

A number of review papers have surfaced in recent years looking into classification and feature extraction techniques for accelerometry data [Preece et al. (2009); Yang and Hsu (2010)]. Due to differences in devices and study parameters, it is difficult to directly compare the studies covered in these review papers, but it is informative to see what techniques have been used successfully for classification of different PA types. For example, walking can be identified using a frequency-domain analysis using variation in acceleration and dominant frequency peak between 1-3Hz in the signal spectrum [Karantonis et al. (2006); Ohtaki et al. (2005)]. To distinguish between walking on level ground and climbing stairs, the discrete wavelet transform can be used [Sekine et al. (2000)]. Classification schemes used include k -nearest neighbor (kNN) [Bussmann et al. (1998); Foerster et al. (1999)], support vector machines (SVM) [Lau et al. (2009); Mannini et al. (2013); Zhang et al. (2006)], Naive Bayes classifier [Huynh and Schiele (2006); Long et al. (2009)], Gaussian mixture models (GMM) [Allen et al. (2006)], hidden Markov models (HMM) [Mannini and Sabatini (2010); Pober et al. (2006)], classification trees [Zhang et al. (2012)], and a combination of methods [Ravi et al. (2005)]. As Xiao et al. (2016) points out, most of these techniques suffer from the fact that the prediction process is difficult to understand and interpret leading to potentially good classifiers without a true understanding of the underlying mechanism. In contrast, our proposed method is simple to understand, and can inform researchers of the underlying mechanisms that differentiate

between types of walking. In addition, many of the current studies combine all types of walking into one category as opposed to differentiating between walking on level ground and climbing stairs. Due to the similarities of these activities, it becomes a much more difficult problem to solve. Also, the EE estimates during walking are inaccurate when locomotion is not on a level ground [Yang and Hsu (2010)].

The rest of the paper is organized as follows. In Section 4.2, we describe the signal processing techniques used and describe the features extracted in detail. In Section 4.3, we detail the proposed normalization technique, and we review the classification model used. In Section 4.4, we evaluate the classification models under different conditions of sensor location and window size. In addition, we evaluate relevant features and detail the relevant feature differences across the different conditions. In Section 4.5, we conclude our paper with a discussion about the limitations of our study, and describe future study considerations.

4.2 Signal processing

We start with the original triaxial signal $\mathbf{x}_i(t) = \{x_i(t), y_i(t), z_i(t)\}$, where $x_i(t)$, $y_i(t)$, and $z_i(t)$ denote the acceleration measurements for subject i at time t from the three orthogonal axes. The interpretation of the acceleration measurements along these three axes depends on the orientation of the device with respect to gravity. In order to remove the effects of orientation from signal, we extract most of our features from the vector magnitude, VM , of the signal defined as:

$$VM_i(t) = \sqrt{x_i(t)^2 + y_i(t)^2 + z_i(t)^2} \quad (4.1)$$

We use a sliding window of differing lengths (2.56, 5.12, and 10.24 seconds) in order to extract features. Figure 4.2 displays sample windows of 10.24 seconds for the three walking activities for a single subject. We can see that walking and stair walking have nice periodic properties which can be described nicely using a frequency analysis approach. These features are preserved in the transformed VM signal as well. For this reason, we utilize the FFT and DWT of the VM to extract the majority of our features from the frequency domain.

The sliding window FFT of a signal $x(t)$ is defined as

$$X(f, t) = \sum_{u=[t-\tau/2]}^{[t+\tau/2]} x(u)h(u)e^{-i2\pi fu/\tau} \quad (4.2)$$

where f is the frequency index and the weights $h(u)$ assign more weight to observations close to t . We use the weights defined by the Hanning window, $h(u; \tau) = 0.5[1 - \cos\{2\pi u/(\tau - 1)\}]$, as they have been shown to reduce aliasing, or blurring of the spectrum [Urbanek et al. (2015)]. The DWT of a signal $x(t)$ is defined as

$$x(n) = \sum_{j=1}^J \sum_{k \in \mathbb{Z}} d_j(k)\psi^*(n - 2^j k) + \sum_{k \in \mathbb{Z}} a_j(k)\phi(n - 2^j k) \quad (4.3)$$

where $j \in \mathbb{Z}$ and $k \in \mathbb{Z}$ represent the resolution, J is the depth of level, ψ is the reconstruction wavelet function and ϕ is the scaling function [Sekine et al. (2000)]. The wavelet coefficients d_j represent the details of the original signal at different levels of the decomposition, and the a_j represent the approximation of the original signal. The wavelet coefficient d_j and scaling coefficient a_j are given by

$$a_j(n) = \sum_k g(k - 2^j n) a_{j-1}(k) \quad (4.4)$$

$$d_j(n) = \sum_k h(k - 2^j n) a_{j-1}(k) \quad (4.5)$$

where g and h represent coefficients of the low-pass and high-pass filters, respectively. In addition to the frequency domain, we also extract features from the VM and raw triaxial signal in the time domain.

4.2.1 Frequency domain features

Figure 4.3 shows the spectra obtained from the FFT (left column) and the wavelet coefficients obtained from the DWT (right column) for the 10.24 second windows of VM displayed in the right column of Figure 4.2. In the following paragraphs, we define each of the frequency domain features derived from these transformations of the VM .

There are four features derived from the FFT. A subject's cadence (steps per second) is defined as the dominant frequency (**f1**) in the FFT spectrum between 1.2 Hz and 4.0 Hz. The **ratio.VM** is defined as the ratio of the partial area under the spectrum related to frequencies of walking to the total area under the spectrum as defined in Urbanek et al. (2015) and Straczekiewicz et al. (2016). The **p1** is the partial area under the peak in the power spectrum located at **f1**. The **p1_TP** is defined as the ratio of **p1** to the total area under the power spectrum between 0.3 Hz and 12.5 Hz. Figure 4.4 provides a visual representation of these features.

In addition, there are two features derived from the DWT similar to those described in Zhang et al. (2012). They are given by the following equations:

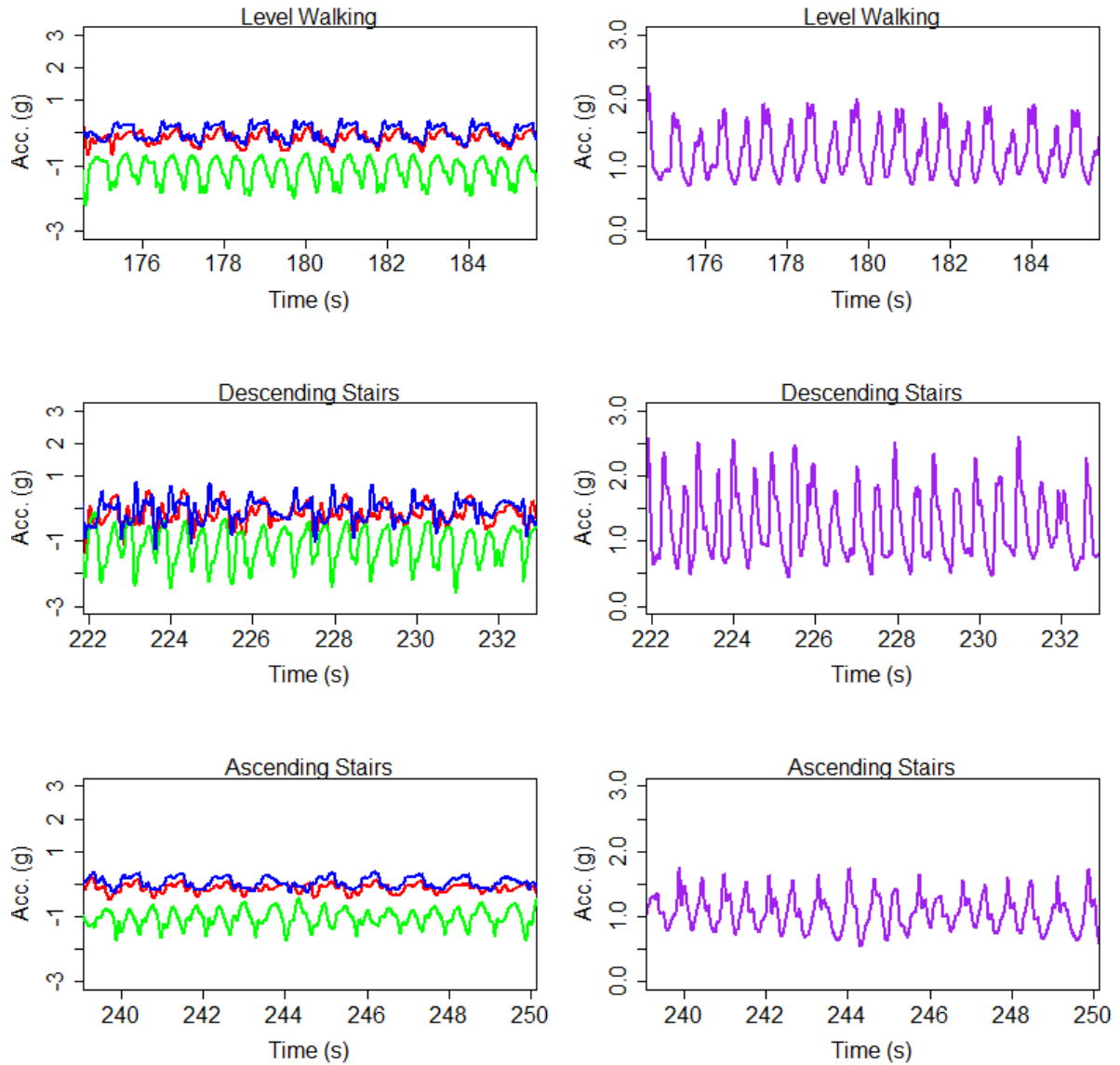


Figure 4.2: Raw triaxial acceleration signal with different colors representing data from each axis (left column) and vector magnitude (right column) for 10 seconds of level walking (top row), descending stairs (middle row), and ascending stairs (bottom row) for a single subject's data collected at the left wrist.

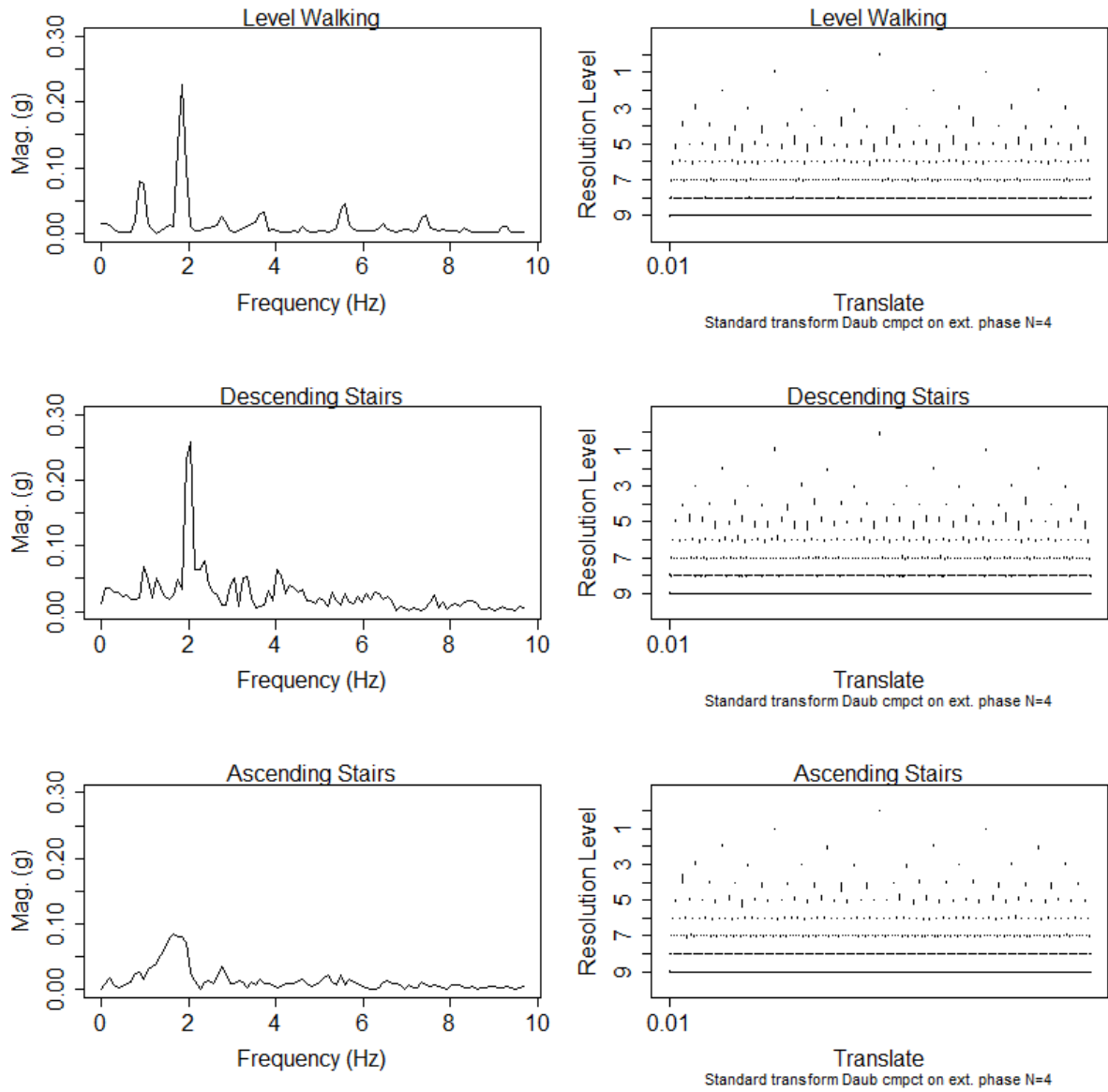


Figure 4.3: Fourier spectra (left column) and wavelet decomposition (right column) for 10 seconds of level walking (top row), descending stairs (middle row), and ascending stairs (bottom row) for a single subject's data collected at the left wrist.

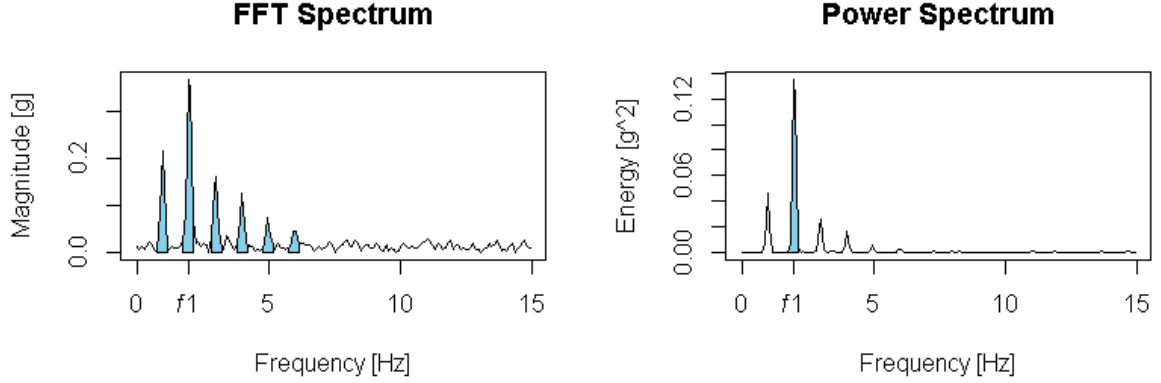


Figure 4.4: Fourier spectrum (left) and power spectrum (right) with shaded regions describing the features derived from the FFT. In the left figure, the shaded region represents the numerator of **ratio.VM**, and the dominant frequency is labeled as **f1**. In the right figure, the shaded region represents **p1**.

$$DWT_VM2 = \sum_{j=\alpha}^{\beta} d_j^2 / VM^2 \quad (4.6)$$

$$DWT_TP = \sum_{j=\alpha}^{\beta} d_j^2 / \sum_{j=1}^J d_j^2 \quad (4.7)$$

where $d_j^2 = d_j^T d_j$ is the sum of squared DWT coefficient vector of VM at level j ($j = 1, \dots, J$). In addition, VM^2 is the sum of the squared VM signal in each window. For our purposes, we selected α and β to cover the frequency range 0.78-6.25Hz, and J was selected to cover the frequency range 0-12.5Hz. DWT_VM2 measures the ratio of the power of wavelet coefficients in the frequency range for walking to the total power of the signal and DWT_TP measures the ratio of the power of wavelet coefficients in the frequency range for walking to the total power of all wavelet coefficients in frequency range associated with human movement. For example, the numerator for both DWT features would be computed as the sum of the

squared coefficients from decomposition levels 4 to 6 in the right column of Figure 4.3.

4.2.2 Time domain features

In addition to the FFT and DWT features, we also included vector magnitude count (*VMC* [Straczkiewicz et al. (2016); Urbanek et al. (2015)] defined as the mean absolute deviation of the *VM* and given by

$$VMC(t) = \frac{1}{\tau} \sum_{u=[t-\tau/2]}^{[t+\tau/2]} |vm(u) - \frac{1}{\tau} \sum_{u=1}^{\tau} vm(u)|, \quad (4.8)$$

and four features derived from the raw triaxial signal: activity intensity ($ActInt = (s_x + s_y + s_z)/3$), $Corr(XY)$, $Corr(XZ)$, and $Corr(YZ)$. Where

$$Corr(XY) = \frac{1}{n-1} \sum_{i=1}^n \left(\frac{x_i - \bar{x}}{s_x} \right) \left(\frac{y_i - \bar{y}}{s_y} \right) \quad (4.9)$$

is the Pearson correlation coefficient between the x and y axes and is defined similarly for $Corr(XZ)$ and $Corr(YZ)$.

4.3 Methods

4.3.1 Feature normalization

Before training and testing any population level classification model, it is important to normalize features at the subject level. As Xiao et al. (2016) demonstrated, accelerometry data is not directly comparable across subjects. Figure 4.5 illustrates these subject to subject differences for the *VM* for a 10.24 second window of each walking activity for two subjects from our study. While the measured acceleration

appear similar in nature, we can see that the magnitude of the signal for each activity is different across the two subjects. However, we observe that the magnitude of the signal for descending stairs is the highest followed by level walking and then ascending stairs. Hence our motivation for normalization is to normalize all features to walking. The usual standardization simply centers data around the mean of the distribution and scales by the overall standard deviation. In Figure (density plots of features) we observe that the distribution of these features at best follow a mixture of normal distributions, and therefore the usual standardization is not appropriate. An assumption that we will make is that level walking is the overwhelming dominant type of walking for the vast majority of human physical activity. Therefore, we explore a simple, yet novel normalization scheme of centering each feature around the median value and scaling by the median absolute deviation (MAD). For a feature x , calculate a pseudo z-score as

$$z^* = \frac{x - \text{median}(x)}{MAD(x)} \quad (4.10)$$

Standardizing the features in this way ensures that each z-score can be interpreted as a deviation from level walking. In order to evaluate the performance of such normalization, all models were trained and tested using the non-standardized features in addition to our proposed normalization.

4.3.2 Classification model

All modeling was performed using RStudio version 0.99.467 [RStudio Team (2015)]. We extend our previous work in Chapter 3 where we used classification trees to build

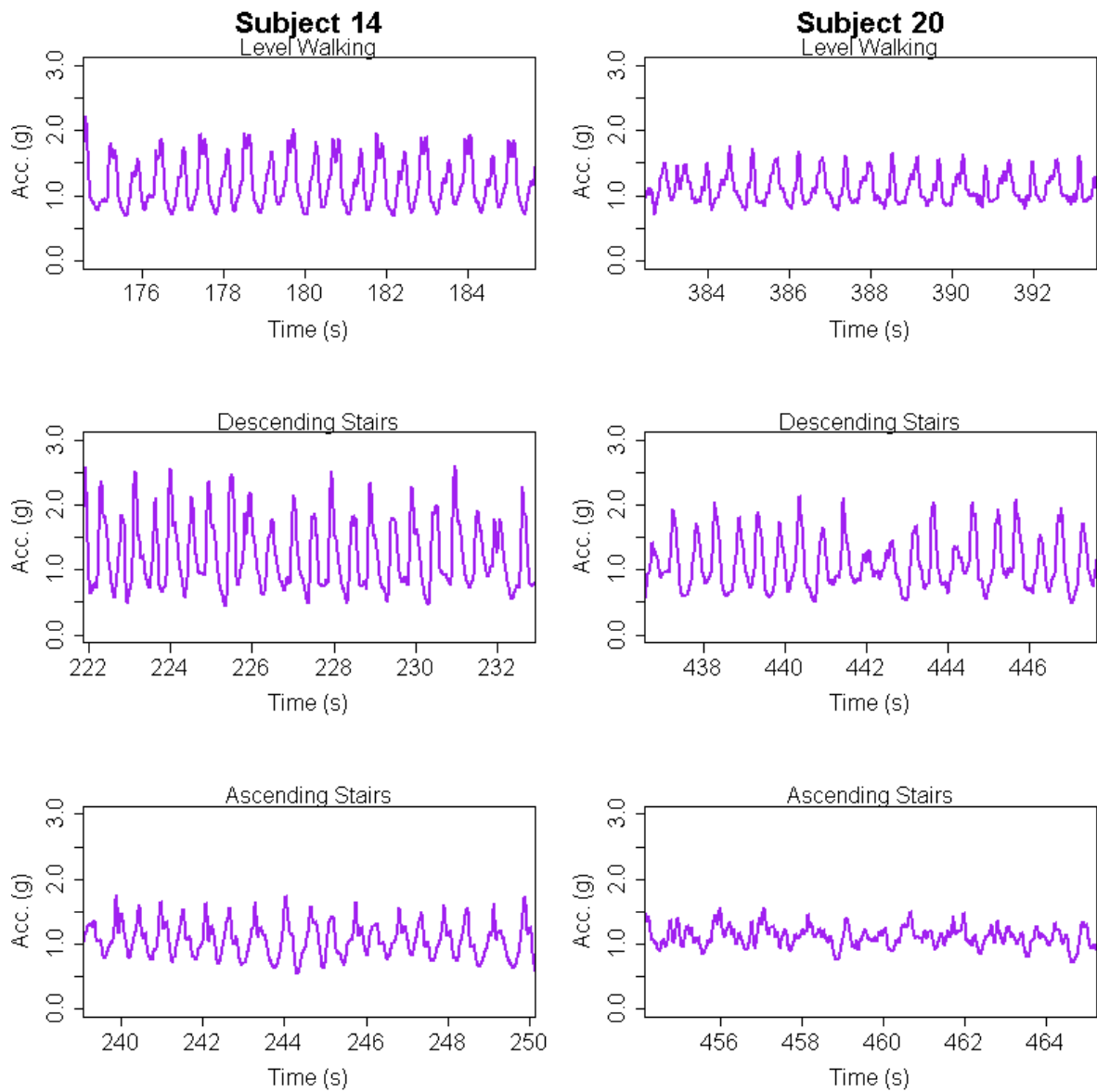


Figure 4.5: Vector magnitude for 10.24s windows of level walking (top row), descending stairs (middle row), and ascending stairs (bottom row) for Subject 14 (left column) and Subject 20 (right column).

subject specific classification models in order to have interpretable models that may inform the choice of predictors in subsequent association studies of walking with certain health related outcomes. The classification tree methodology from the R package **rpart** was used for fitting of all models [Therneau and Atkinson (2015); Therneau et al. (2015)].

In order to evaluate the performance of each classifier, cross-validation (CV) was implemented to investigate the accuracy. For performance evaluation, the subjects' data were split into training (20 subjects) and testing (11 subjects) datasets. Each model was fit to the training data and pruned using the 1-SE rule [Therneau and Atkinson (2015)]. The model was then tested on the remaining 11 subjects' data. This process was repeated 100 times for each combination of sensor location and window length. Final models were fit to all subjects' data using a uniform class prior to address the imbalance in the three activities.

In addition to classification rates, we evaluated the feature set to identify which predictors provided the best separation of the three walking activities. At each iteration, we assigned a rank to the variable importance produced by the model, and then we averaged these rankings across all iterations. The rankings ranged from 1 to 13 for the most important to least important features, respectively.

4.4 Results

We applied the methods described in Section 4.3 to the data from the IUWDS described in Section 4.1.1. The classification results are displayed in Figures 4.6 and 4.7 in terms of sensitivity, specificity, positive predictive value, and F1 score. The final classification models and confusion matrices for each of the 12 scenarios for the

proposed method are provided in Appendix 4.6.

Figure 4.6 shows the sensitivity and specificity obtained through RCV for the 12 classification models for both normalized and raw feature models. Because of the imbalance in the three activities, we observe very high sensitivity for walking, but we observe much lower sensitivity for ascending and descending stairs regardless of sensor location and window size. In addition, we see the normalized features outperform the raw features in nearly every scenario. Figure 4.7 shows the PPV and F1 score for the 12 classification models for both the normalized and non-normalized feature models. Again, we notice the normalized features results are nearly always better than the results obtained using the raw features. Similar to what we observed in Chapter 3, walking on level ground is the easiest activity to identify among the three types of walking, but it is also the most prevalent activity by a large margin. Instead, if we focus on the PPV in the top panel of Figure 4.7, we observe that the PPV is higher for left wrist versus left hip for descending stairs while the relationship is reversed (i.e., left hip higher than left wrist) for ascending stairs. The left and right ankles yield nearly identical results in terms of model performance.

Figure 4.8 shows the feature importance for the 12 scenarios of window length and sensor location. Similar to what we observed in our previous work in Chapter 3, we see that for data collected from the left wrist, the most important features are those features which measure the variation in measured acceleration (i.e. $SD(VM)$, VMC , DWT_VM2 , $ActInt$, and $p1$). For the data collected at the hip, the same five features are ranked the highest with exception that $ratio.VM$ becomes the most important variable for window lengths of 10.24 seconds. This is most likely attributable to the need for higher resolution of the walking spectra before $ratio.VM$ can be accurately

measured. Consistently, $p1$ and $p1_{TP}$ are ranked highly for the models built from ankle data. This is consistent to our previous findings at the subject level, and indicate the magnitude of the walking spectra at the dominant frequency is quite useful for differentiating between types of walking when data is collected at the ankle.

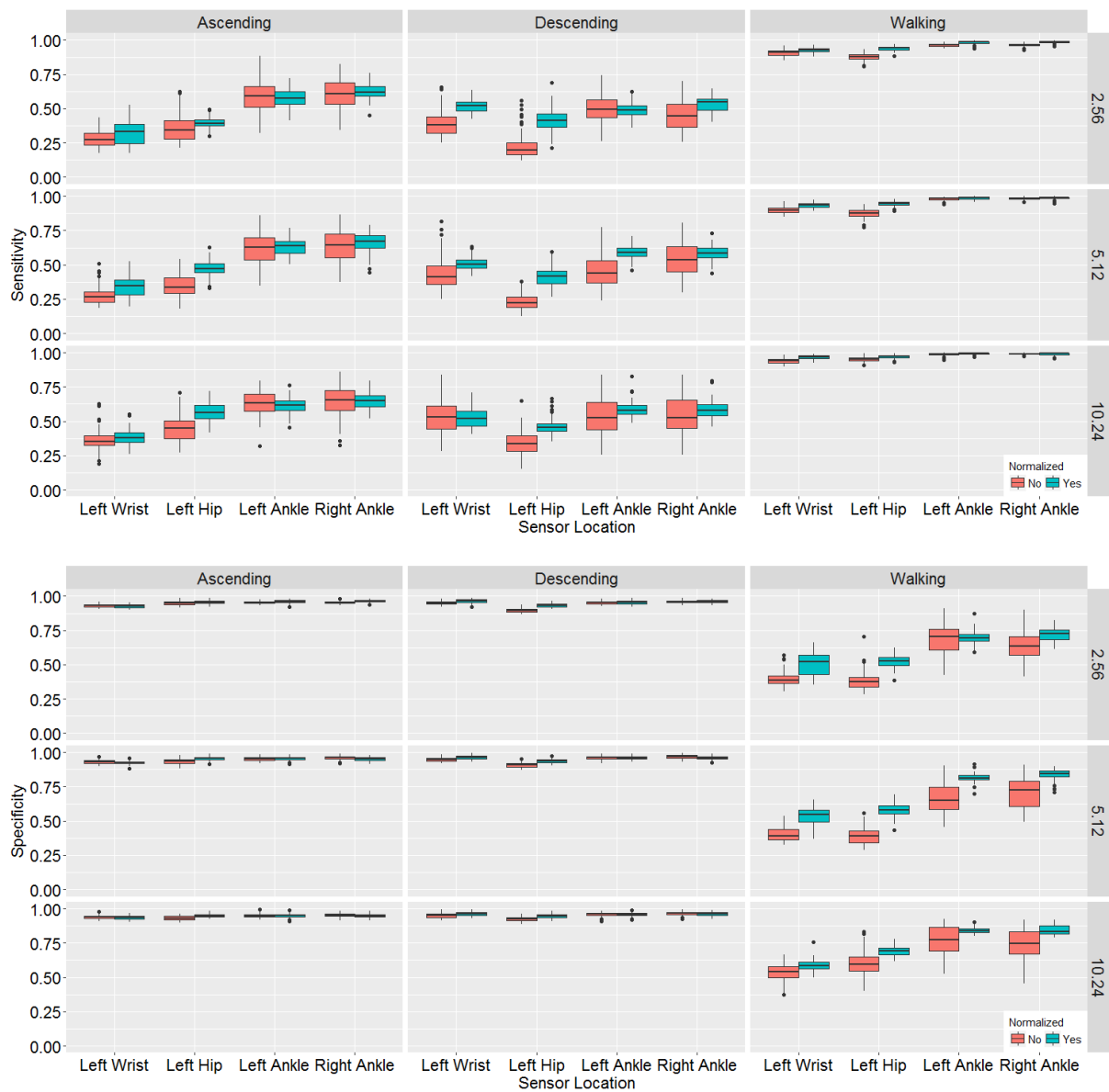


Figure 4.6: Sensitivity and specificity by activity, sensor location, and window length.

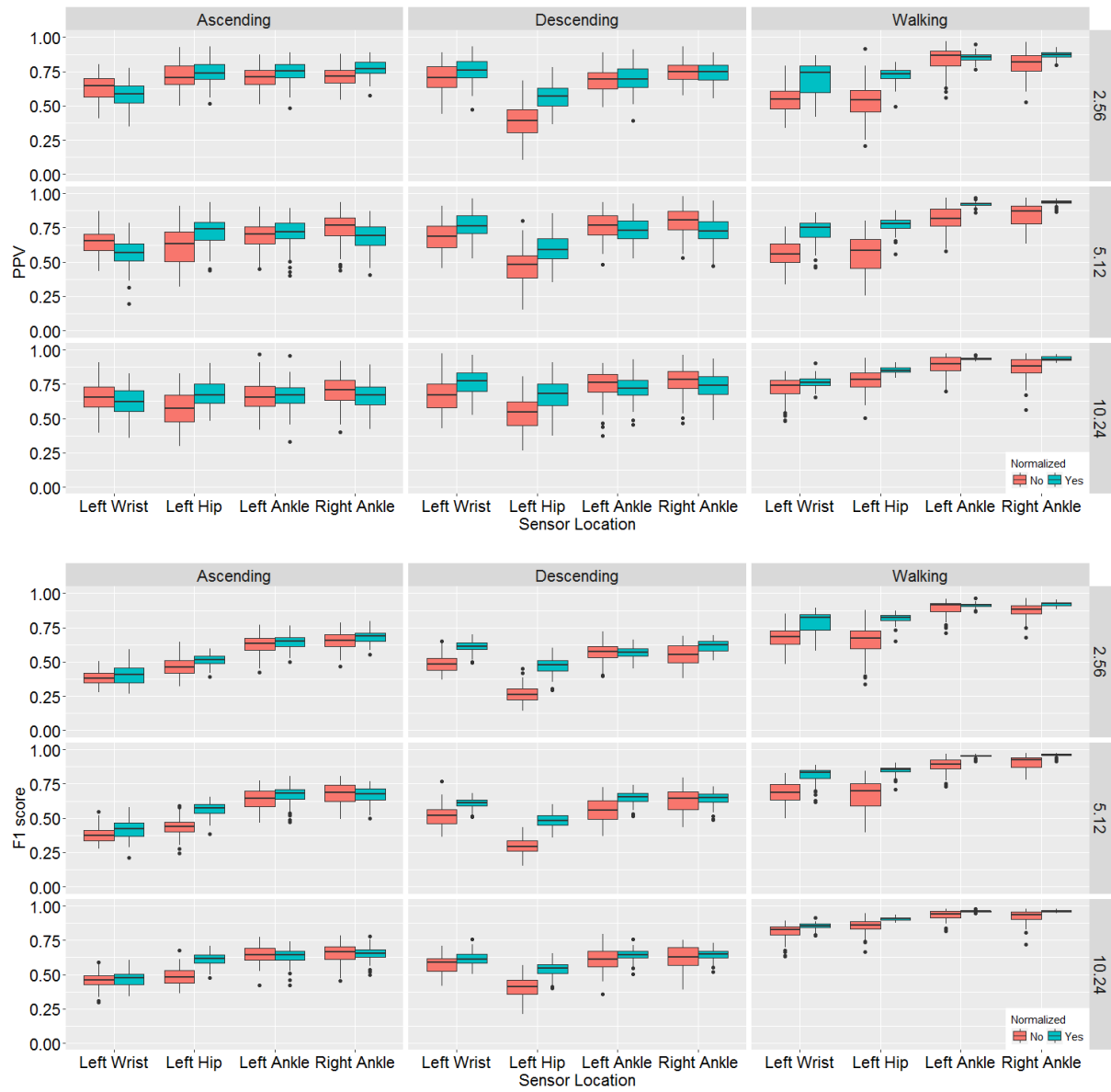
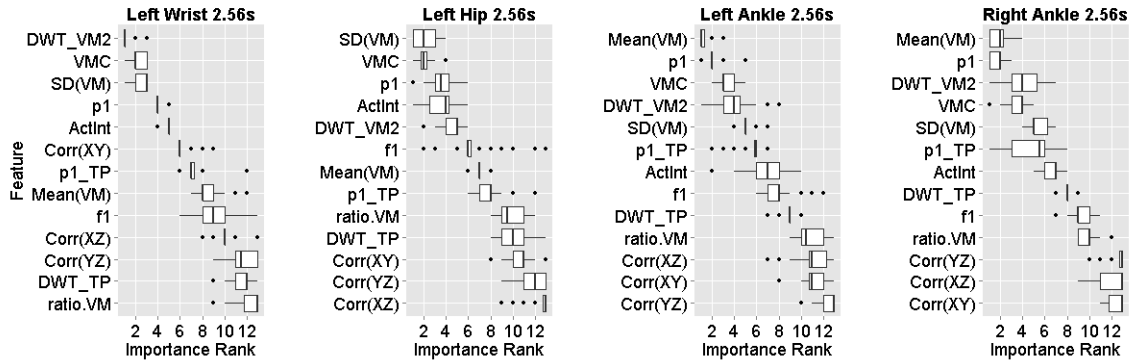
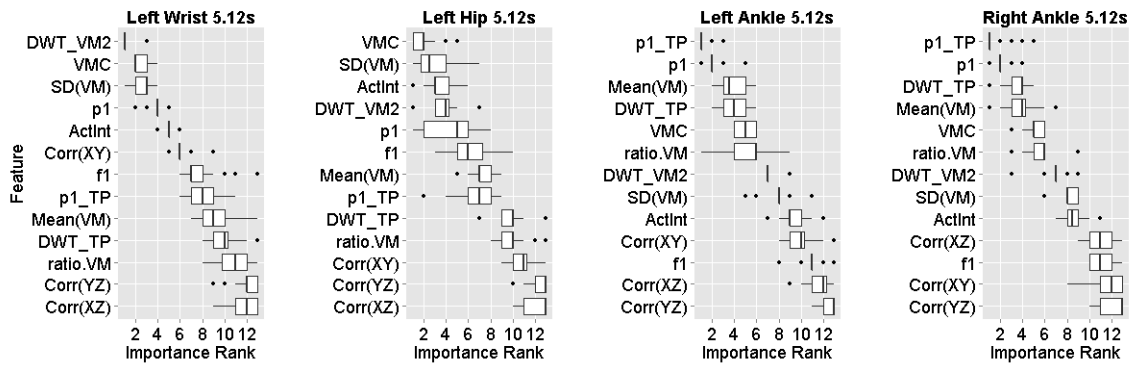


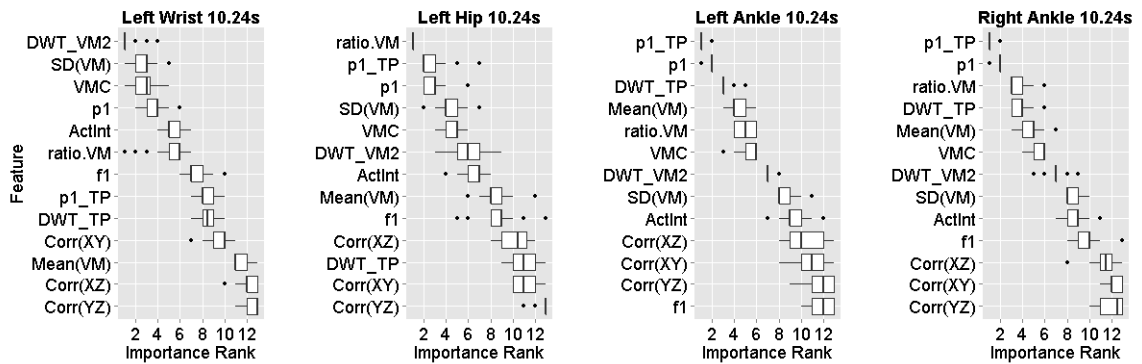
Figure 4.7: Positive predictive value and F1 score by activity, sensor location, and window length.



(a)



(b)



(c)

Figure 4.8: Variable importance rankings for the twelve scenarios. Variables are sorted from top to bottom by median importance rank.

4.5 Discussion

We have proposed a classification tree-based method for differentiating between walking on level ground, ascending stairs, and descending stairs using accelerometry data. Relevant features were extracted from the raw data using a combination of frequency analysis features and time domain features and a range of window sizes (e.g., 2.56, 5.12, and 10.24 seconds). In Chapter 3, we showed that we can achieve very good classification results using the proposed methods for classification within subjects. In this chapter, we have taken a step forward in trying to build a population level classification model under a number of window size and sensor location combinations. We proposed a novel normalization of features to standardize all activities to walking.

The within subject methods described in Chapter 3 are more accurate, but in larger scale studies, it may not be feasible to obtain training data for every subject. The population level model detailed in this chapter serve as an important step towards our ultimate goal of building a reliable classification model. We showed that a novel, yet simple, normalization of the features can improve between subject classification results in nearly all scenarios and activities.

The data from the IUWDS was collected in a simulated free-living environment from relatively healthy adults ranging in age from 23 to 54 years. The large heterogeneity in the study population, with respect to age, BMI, and gender, gives value to the generalizability of our results. A next step for this research will certainly include looking at smaller groups of homogeneous individuals to assess the accuracy of more population specific models. In addition to homogeneous groups, more sophisticated normalization techniques, or combinations of techniques, may improve the accuracy

of the proposed models.

4.6 Acknowledgements

This paper was made possible, in part, with support from the Indiana Clinical and Translational Sciences Institute Design and Biostatistics Pilot Grant funded, in part by Grant UL1TR001108, from the National Institutes of Health, National Center for Advancing Translational Sciences, Clinical and Translational Sciences Award. J Harezlak has received funding from the National Institute of Mental Health research grant R01MH108467.

Appendix 4.A Final population trees and CV confusion matrices

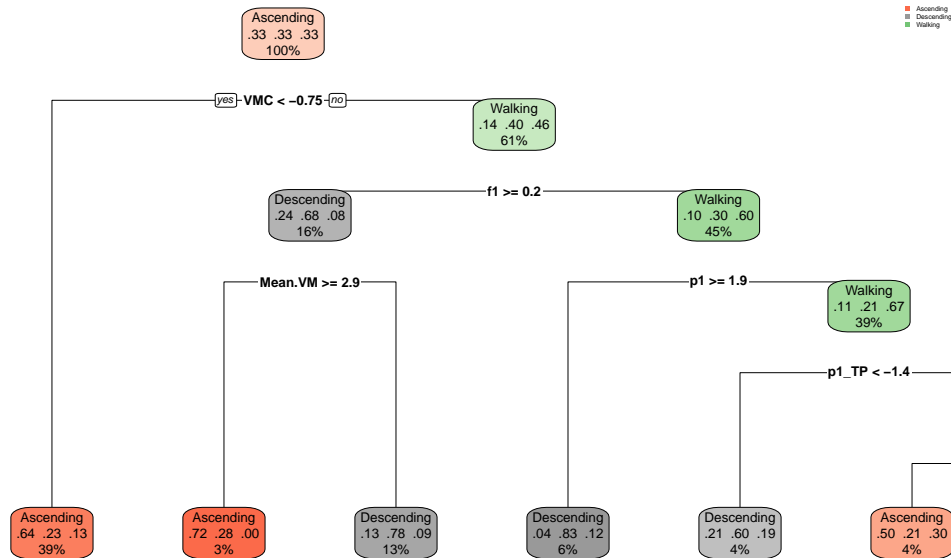


Figure 4.9: Final classification tree for data collected at the hip and features extracted using 2.56 second windows.

Table 4.1: Classification results based on data collected at the hip and features extracted using 2.56 second windows.

Summary			
Overall Accuracy		70.8%	
Confusion Matrix – HIP 2.56s			
Actual activity class			Classified as
Ascending	Descending	Walking	
71,675	24,873	85,717	Ascending
14,392	51,746	62,065	Descending
9,941	15,572	392,876	Walking

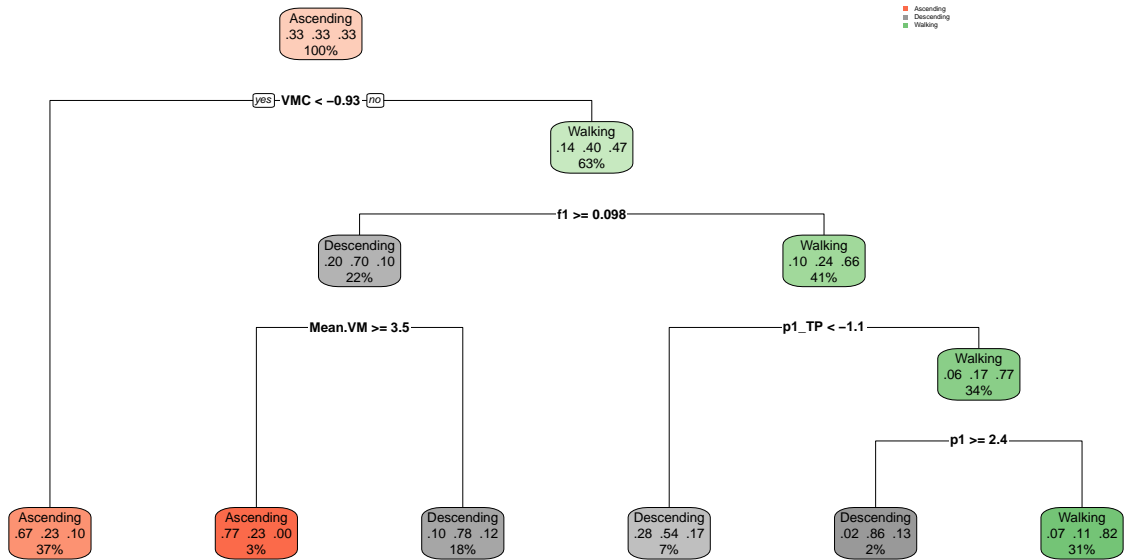


Figure 4.10: Final classification tree for data collected at the hip and features extracted using 5.12 second windows.

Table 4.2: Classification results based on data collected at the hip and features extracted using 5.12 second windows.

Summary			
Overall Accuracy		74.5%	
Confusion Matrix – HIP 5.12s			
Actual activity class			Classified as
Ascending	Descending	Walking	
69,828	22,811	57,338	Ascending
17,167	54,647	63,633	Descending
9,116	14,339	414,143	Walking

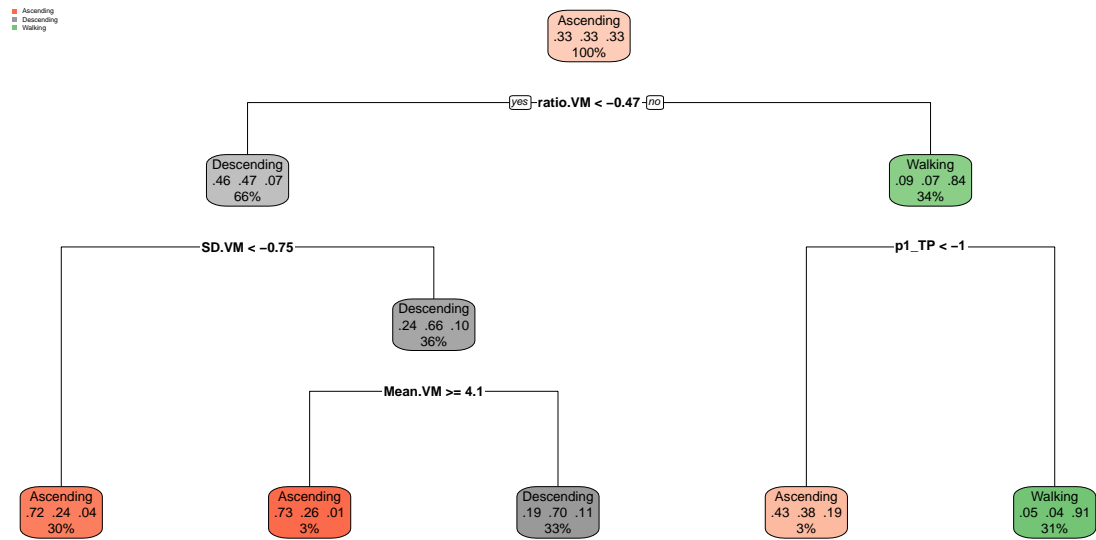


Figure 4.11: Final classification tree for data collected at the hip and features extracted using 10.24 second windows.

Table 4.3: Classification results based on data collected at the hip and features extracted using 10.24 second windows.

Summary			
Overall Accuracy			80.5%
Confusion Matrix – HIP 10.24s			
Actual activity class			Classified as
Ascending	Descending	Walking	
64,608	23,417	28,118	Ascending
24,350	61,817	50,587	Descending
6,549	7,043	451,442	Walking

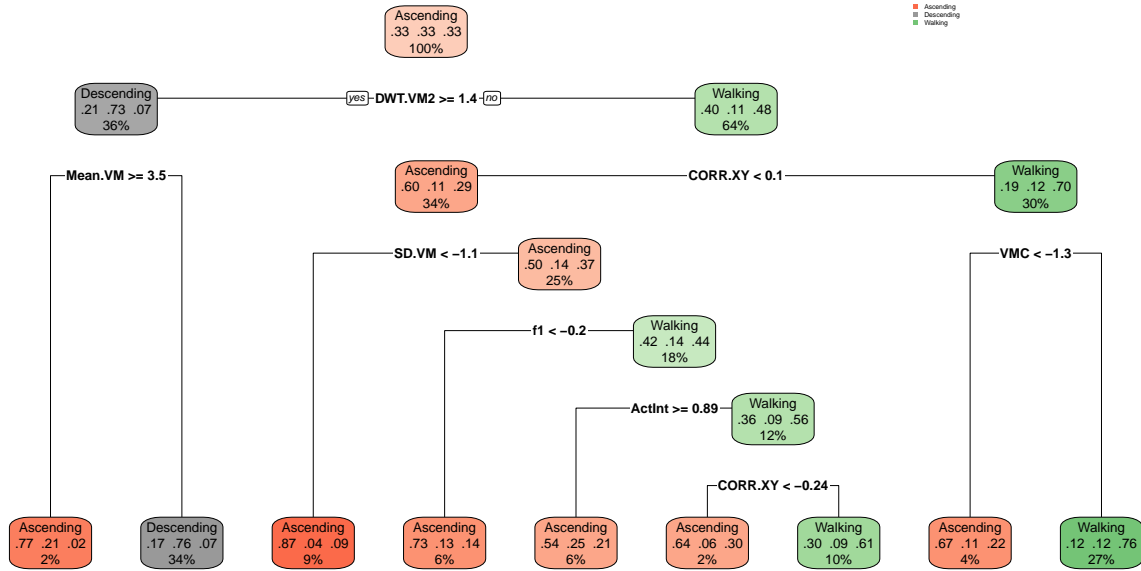


Figure 4.12: Final classification tree for data collected at the left wrist and features extracted using 2.56 second windows.

Table 4.4: Classification results based on data collected at the left wrist and features extracted using 2.56 second windows.

Summary			
Overall Accuracy		69.2%	
Confusion Matrix – Left Wrist 2.56s			
Actual activity class			Classified as
Ascending	Descending	Walking	
55,658	12,012	115,963	Ascending
19,468	70,010	46,442	Descending
20,882	10,169	378,253	Walking

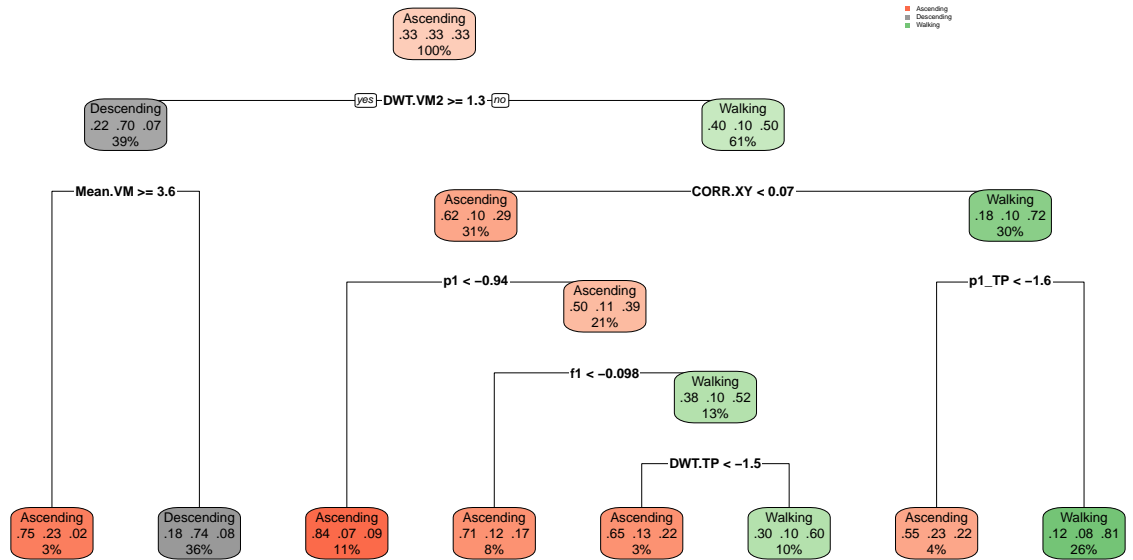


Figure 4.13: Final classification tree for data collected at the left wrist and features extracted using 5.12 second windows.

Table 4.5: Classification results based on data collected at the left wrist and features extracted using 5.12 second windows.

Summary			
Overall Accuracy		70.7%	
Confusion Matrix – Left Wrist 5.12s			
Actual activity class			Classified as
Ascending	Descending	Walking	
54,520	13,478	101,146	Ascending
21,386	70,474	47,792	Descending
20,205	7,845	386,176	Walking

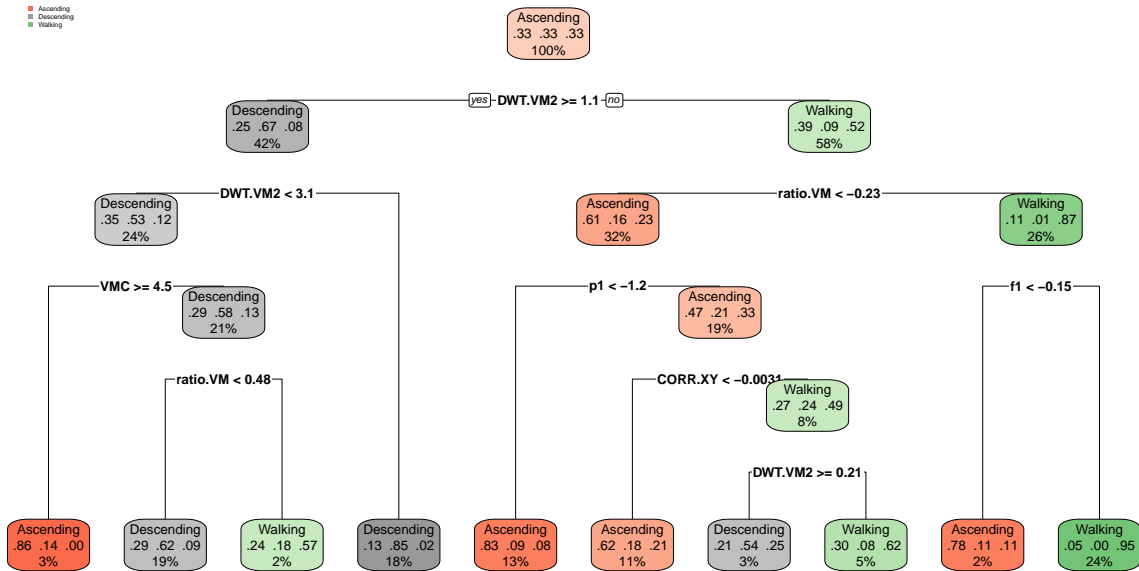


Figure 4.14: Final classification tree for data collected at the left wrist and features extracted using 10.24 second windows.

Table 4.6: Classification results based on data collected at the left wrist and features extracted using 10.24 second windows.

Summary			
Overall Accuracy		74.7%	
Confusion Matrix – Left Wrist 10.24s			
Actual activity class			Classified as
Ascending	Descending	Walking	
60,062	17,775	82,446	Ascending
24,777	70,375	42,164	Descending
10,668	4,127	405,537	Walking

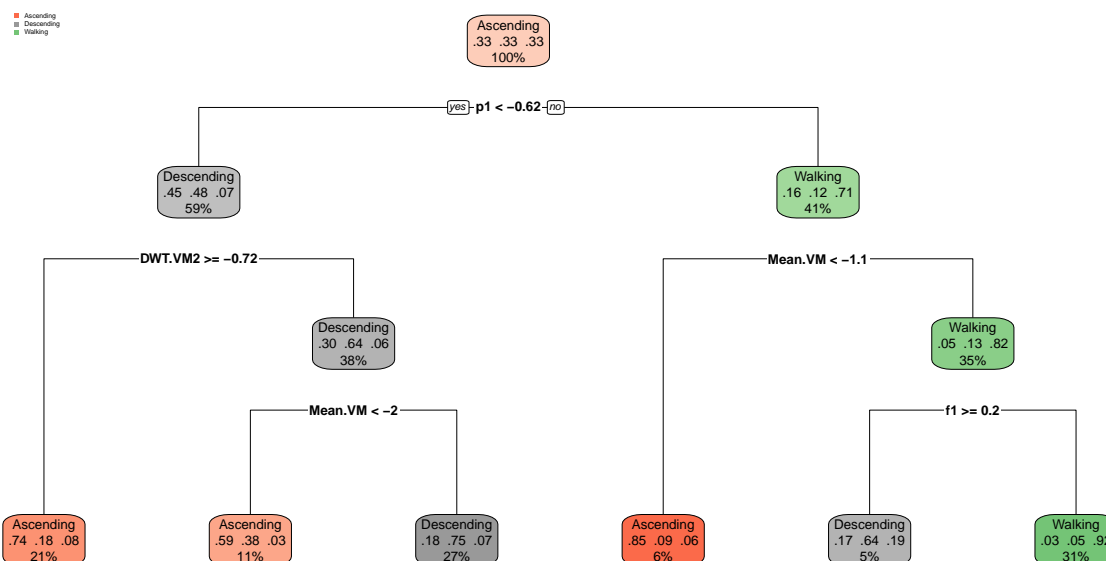


Figure 4.15: Final classification tree for data collected at the left ankle and features extracted using 2.56 second windows.

Table 4.7: Classification results based on data collected at the left ankle and features extracted using 2.56 second windows.

Summary			
Overall Accuracy		82.0%	
Confusion Matrix – Left Ankle 2.56s			
Actual activity class			Classified as
Ascending	Descending	Walking	
71,438	21,988	31,660	Ascending
21,762	63,949	46,920	Descending
2,808	6,254	462,078	Walking

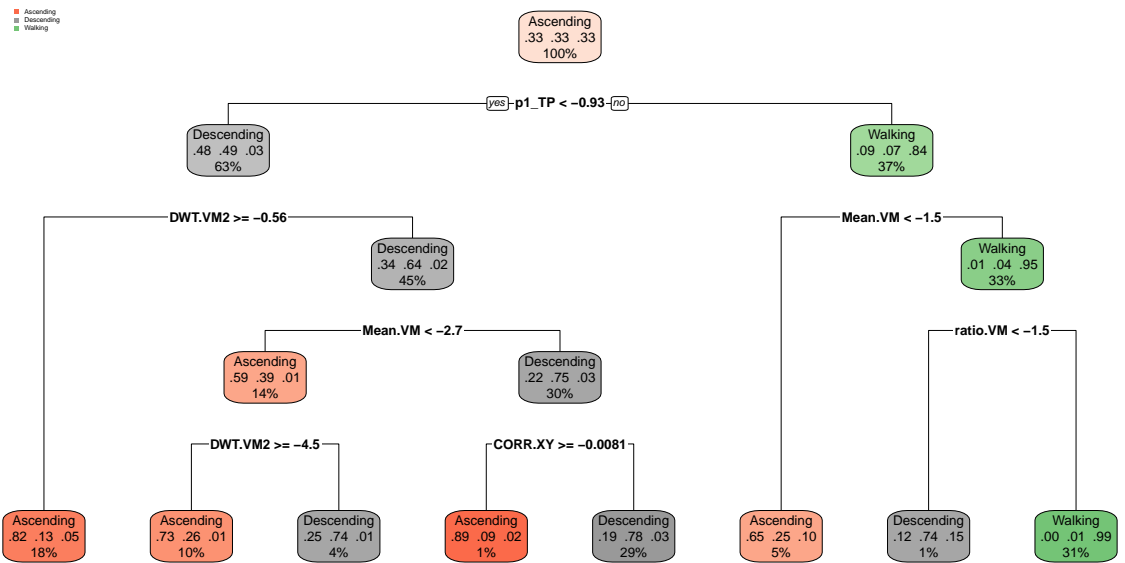


Figure 4.16: Final classification tree for data collected at the left ankle and features extracted using 5.12 second windows.

Table 4.8: Classification results based on data collected at the left ankle and features extracted using 5.12 second windows.

Summary			
Overall Accuracy		87.2%	
Confusion Matrix – Left Ankle 5.12s			
Actual activity class			Classified as
Ascending	Descending	Walking	
68,828	21,287	18,694	Ascending
24,466	66,985	22,044	Descending
2,817	3,525	494,376	Walking

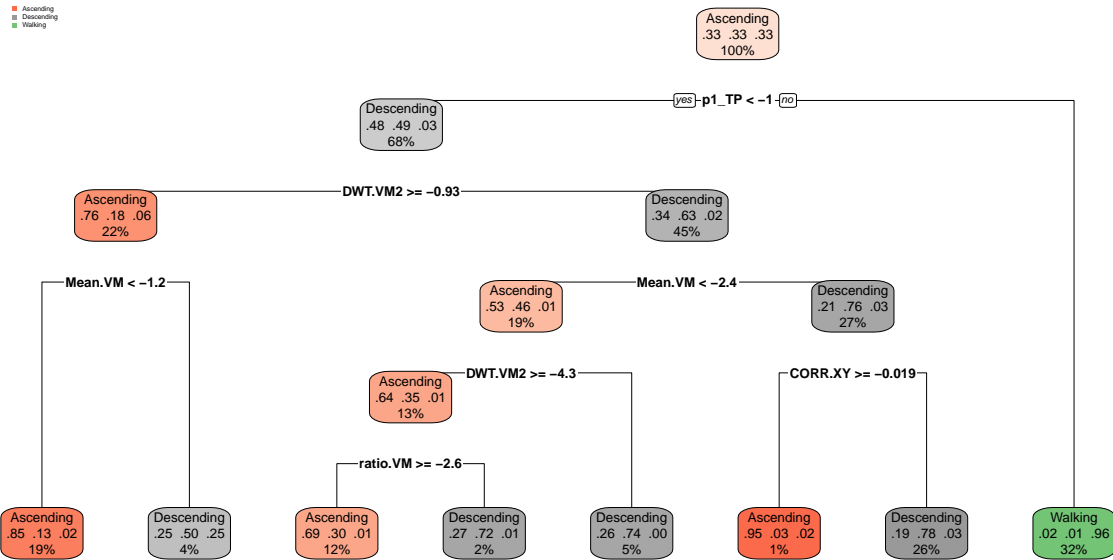


Figure 4.17: Final classification tree for data collected at the left ankle and features extracted using 10.24 second windows.

Table 4.9: Classification results based on data collected at the left ankle and features extracted using 10.24 second windows.

Summary			
Overall Accuracy		87.1%	
Confusion Matrix – Left Ankle 10.24s			
Actual activity class			Classified as
Ascending	Descending	Walking	
63,740	24,603	16,084	Ascending
29,045	66,272	18,544	Descending
2,722	1,402	495,519	Walking

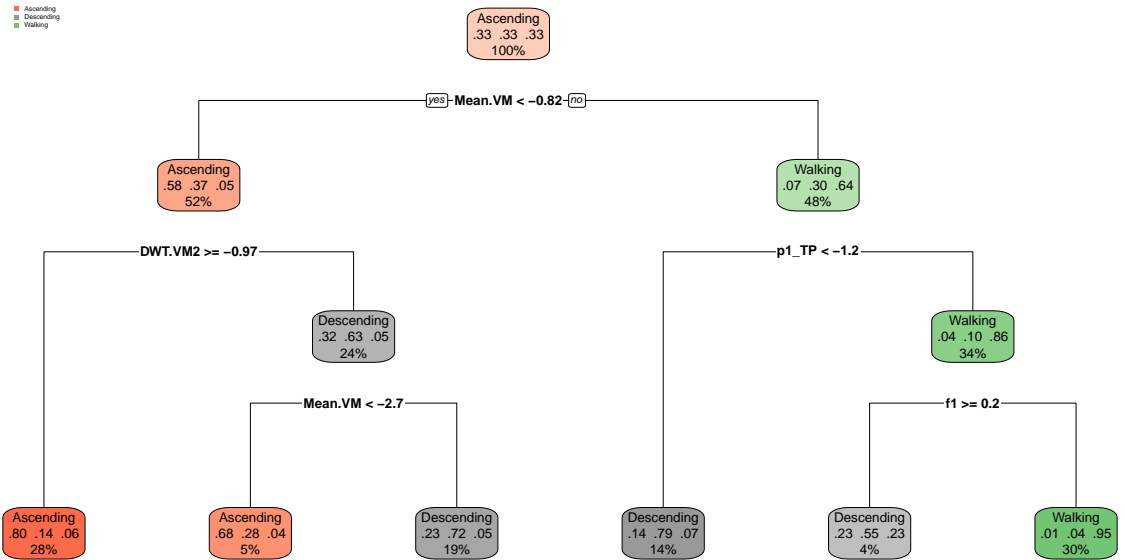


Figure 4.18: Final classification tree for data collected at the right ankle and features extracted using 2.56 second windows.

Table 4.10: Classification results based on data collected at the right ankle and features extracted using 2.56 second windows.

Summary			
Overall Accuracy		84.1%	
Confusion Matrix – Right Ankle 2.56s			
Actual activity class			Classified as
Ascending	Descending	Walking	
74,379	18,292	27,884	Ascending
19,561	68,469	42,801	Descending
2,068	5,430	469,973	Walking

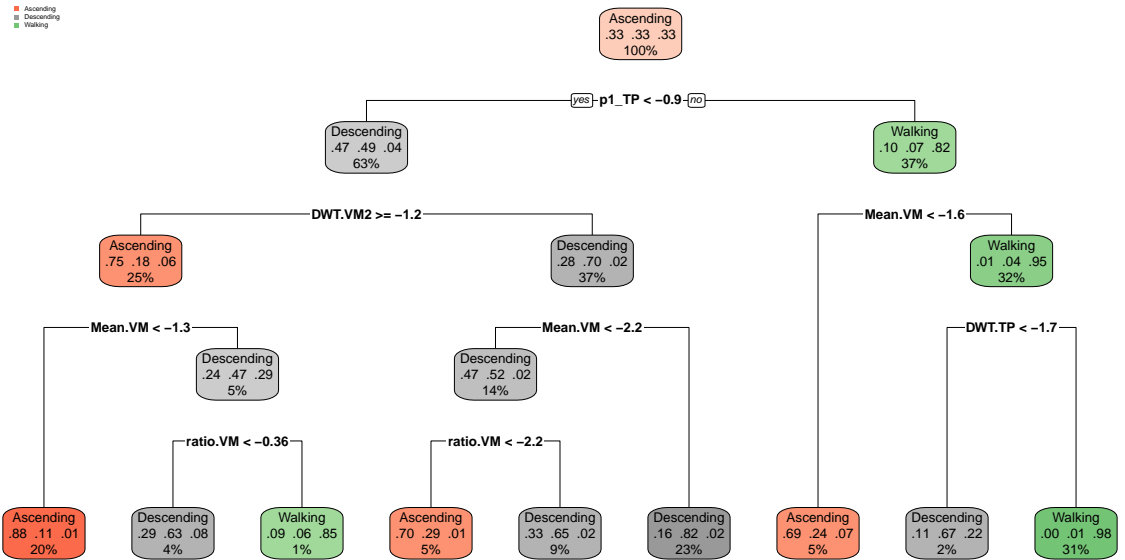


Figure 4.19: Final classification tree for data collected at the right ankle and features extracted using 5.12 second windows.

Table 4.11: Classification results based on data collected at the right ankle and features extracted using 5.12 second windows.

Summary			
Overall Accuracy			87.6%
Confusion Matrix – Right Ankle 5.12s			
Actual activity class			Classified as
Ascending	Descending	Walking	
66,226	21,089	13,268	Ascending
27,201	66,675	21,439	Descending
2,684	4,033	500,407	Walking

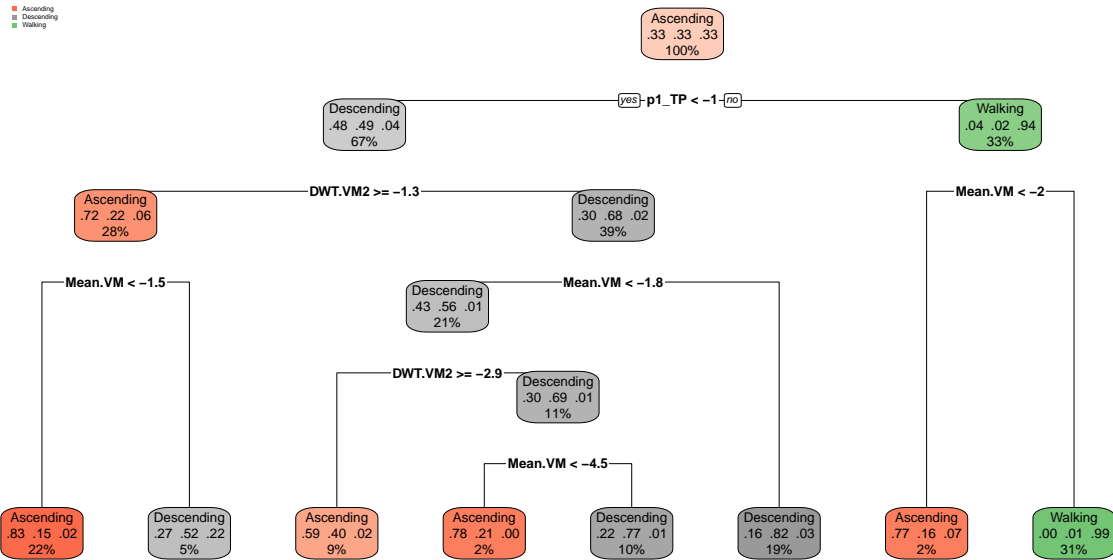


Figure 4.20: Final classification tree for data collected at the right ankle and features extracted using 10.24 second windows.

Table 4.12: Classification results based on data collected at the right ankle and features extracted using 10.24 second windows.

Summary			
Overall Accuracy			87.4%
Confusion Matrix – Right Ankle 10.24s			
Actual activity class			Classified as
Ascending	Descending	Walking	
63,124	22,143	12,688	Ascending
28,908	68,049	21,247	Descending
3,475	2,085	496,212	Walking

Chapter 5

Discussion

Accelerometers are being widely used in PA studies around the world. They are relatively cheap and offer an objective measure of human movement. However, the large amount of raw data collected by these devices are complicated to work with. It is often necessary to reduce the dimensions of the raw data using signal processing methodology, and different types of PA are best described by different sets of features. Further, subject to subject variability makes it impossible to compare the raw data or features extracted from the raw data without an effective normalization.

My dissertation addresses these challenges in Chapters 2, 3, and 4. Specific emphasis is placed on the extensive data processing required before any modeling can occur. In Chapter 2, we provided a framework for extracting characteristics of walking from the raw accelerometry data and used a novel application of functional regression models to associate walking with specific health related outcomes (e.g., age and BMI). The methodology could be applied in a more clinical setting to track changes in walking characteristics as degenerative diseases (e.g., Parkinson's disease) progress. In Chapters 3 and 4, we evaluated the classification accuracy of models built from data collected from a number of sensor location and processing scenarios. In Chapter 3, we demonstrated that we can achieve high classification accuracy when differentiating between walking and stair climbing at the subject level. We also provided feature evaluation to determine what features provide the best discrimination under

the different scenarios. In Chapter 4, we demonstrated challenge of building a population level classification model under the same scenarios described in Chapter 3 and provided a novel solution to the problem. My research has also demonstrated the need for careful design of studies using accelerometers. Researchers must consider where to place the device and how to process the resulting data in order to achieve their specific aims.

Further work is needed in the area of accelerometry research. As more data are collected in clinical and observational settings, methodology must be developed and adapted from other areas to address the specific research needs. For example, improved estimation of gait parameters from could help to cut costs as well as improve potential classification models. The area of data normalization also needs much more attention. We addressed normalization in a very specific setting, but the increasing use of gyroscopes in parallel with accelerometers has shown promise in the area of walking classification [Laudanski et al. (2015)]. The methods described in this dissertation should be extended to include gyroscope data to address the complication of differing sensor orientation between individuals. We have attempted to address this issue in this dissertation, but lack of gyroscope data prevented us from making this logical next step. In addition, combining accelerometry data with GPS data, heart rate measurements, and other possible measures could provide valuable information that is lacking when strictly using accelerometry data.

BIBLIOGRAPHY

- Allen, F. R., E. Ambikairajah, N. H. Lovell, and B. G. Celler (2006). Classification of a known sequence of motions and postures from accelerometry data using adapted gaussian mixture models. *Physiological measurement* 27(10), 935.
- Bai, J., J. Goldsmith, B. Caffo, T. A. Glass, and C. M. Crainiceanu (2012). Movelets: A dictionary of movement. *Electronic journal of statistics* 6, 559.
- Banos, O., J.-M. Galvez, M. Damas, H. Pomares, and I. Rojas (2014). Window size impact in human activity recognition. *Sensors* 14(4), 6474–6499.
- Bao, L. and S. S. Intille (2004). Activity recognition from user-annotated acceleration data. In *International Conference on Pervasive Computing*, pp. 1–17. Springer.
- Baranowski, T. (1988). Validity and reliability of self report measures of physical activity: an information-processing perspective. *Research Quarterly for Exercise and Sport* 59(4), 314–327.
- Bussmann, H. B., P. J. Reuvekamp, P. H. Veltink, W. L. Martens, and H. J. Stam (1998). Validity and reliability of measurements obtained with an” activity monitor” in people with and without a transtibial amputation. *Physical therapy* 78(9), 989.
- Bussmann, J., W. Martens, J. Tulen, F. Schasfoort, H. Van Den Berg-Emons, and H. Stam (2001). Measuring daily behavior using ambulatory accelerometry: the

- activity monitor. *Behavior Research Methods, Instruments, & Computers* 33(3), 349–356.
- Campbell, K. L., P. Crocker, and D. C. McKenzie (2002). Field evaluation of energy expenditure in women using triTrac accelerometers. *Medicine and science in sports and exercise* 34(10), 1667–1674.
- Copeland, J. L. and D. W. Esliger (2009). Accelerometer assessment of physical activity in active, healthy older adults. *Journal of aging and physical activity* 17(1), 17–30.
- Ellis, K., J. Kerr, S. Godbole, J. Staudenmayer, and G. Lanckriet (2016). Hip and wrist accelerometer algorithms for free-living behavior classification. *Medicine and science in sports and exercise* 48(5), 933–940.
- Ermes, M., J. Pärkkä, J. Mäntyjärvi, and I. Korhonen (2008). Detection of daily activities and sports with wearable sensors in controlled and uncontrolled conditions. *IEEE transactions on information technology in biomedicine* 12(1), 20–26.
- Esliger, D. W., A. V. Rowlands, T. L. Hurst, M. Catt, P. Murray, and R. G. Eston (2011). Validation of the genea accelerometer.
- Foerster, F., M. Smeja, and J. Fahrenberg (1999). Detection of posture and motion by accelerometry: a validation study in ambulatory monitoring. *Computers in Human Behavior* 15(5), 571–583.
- Gardner, A. W. and E. T. Poehlman (1998). Assessment of free-living daily physical activity in older claudicants: validation against the doubly labeled water tech-

- nique. *The Journals of Gerontology Series A: Biological Sciences and Medical Sciences* 53(4), M275–M280.
- Grant, P. M., C. G. Ryan, W. W. Tigbe, and M. H. Granat (2006). The validation of a novel activity monitor in the measurement of posture and motion during everyday activities. *British journal of sports medicine* 40(12), 992–997.
- Harris, F. J. (1978). On the use of windows for harmonic analysis with the discrete fourier transform. *Proceedings of the IEEE* 66(1), 51–83.
- He, B., J. Bai, V. V. Zipunnikov, A. Koster, P. Caserotti, B. Lange-Maia, N. W. Glynn, T. B. Harris, and C. M. Crainiceanu (2014). Predicting human movement with multiple accelerometers using movelets. *Medicine and science in sports and exercise* 46(9), 1859–1866.
- Hecht, A., S. Ma, J. Porszasz, R. Casaburi, C. C. R. Network, et al. (2009). Methodology for using long-term accelerometry monitoring to describe daily activity patterns in copd. *COPD: Journal of Chronic Obstructive Pulmonary Disease* 6(2), 121–129.
- Huynh, T. and B. Schiele (2006). Towards less supervision in activity recognition from wearable sensors. In *Wearable Computers, 2006 10th IEEE International Symposium on*, pp. 3–10. IEEE.
- Karantonis, D. M., M. R. Narayanan, M. Mathie, N. H. Lovell, and B. G. Celler (2006). Implementation of a real-time human movement classifier using a triaxial accelerometer for ambulatory monitoring. *IEEE transactions on information technology in biomedicine* 10(1), 156–167.

- Kavanagh, J. J. and H. B. Menz (2008). Accelerometry: a technique for quantifying movement patterns during walking. *Gait & posture* 28(1), 1–15.
- Kundu, M. G., J. Harezlak, and T. W. Randolph (2012). Longitudinal functional models with structured penalties. *arXiv preprint arXiv:1211.4763*.
- Kwapisz, J. R., G. M. Weiss, and S. A. Moore (2011). Activity recognition using cell phone accelerometers. *ACM SigKDD Explorations Newsletter* 12(2), 74–82.
- Lange-Maia, B. S., A. B. Newman, E. S. Strotmeyer, T. B. Harris, P. Caserotti, and N. W. Glynn (2015). Performance on fast-and usual-paced 400-m walk tests in older adults: are they comparable? *Aging clinical and experimental research* 27(3), 309–314.
- Lau, H.-y., K.-y. Tong, and H. Zhu (2009). Support vector machine for classification of walking conditions of persons after stroke with dropped foot. *Human movement science* 28(4), 504–514.
- Laudanski, A., B. Brouwer, and Q. Li (2015). Activity classification in persons with stroke based on frequency features. *Medical engineering & physics* 37(2), 180–186.
- Long, X., B. Yin, and R. M. Aarts (2009). Single-accelerometer-based daily physical activity classification. In *Engineering in Medicine and Biology Society, 2009. EMBC 2009. Annual International Conference of the IEEE*, pp. 6107–6110. IEEE.
- Mannini, A., S. S. Intille, M. Rosenberger, A. M. Sabatini, and W. Haskell (2013). Activity recognition using a single accelerometer placed at the wrist or ankle. *Medicine and science in sports and exercise* 45(11), 2193.

- Mannini, A. and A. M. Sabatini (2010). Machine learning methods for classifying human physical activity from on-body accelerometers. *Sensors* 10(2), 1154–1175.
- Moe-Nilssen, R. and J. L. Helbostad (2004). Estimation of gait cycle characteristics by trunk accelerometry. *Journal of biomechanics* 37(1), 121–126.
- Ohtaki, Y., M. Susumago, A. Suzuki, K. Sagawa, R. Nagatomi, and H. Inooka (2005). Automatic classification of ambulatory movements and evaluation of energy consumptions utilizing accelerometers and a barometer. *Microsystem technologies* 11(8-10), 1034–1040.
- Pachi, A. and T. Ji (2005). Frequency and velocity of people walking. *Structural Engineer* 83(3).
- Parkka, J., M. Ermes, P. Korpiä, J. Mantyjarvi, J. Peltola, and I. Korhonen (2006). Activity classification using realistic data from wearable sensors. *IEEE Transactions on information technology in biomedicine* 10(1), 119–128.
- Pober, D. M., J. Staudenmayer, C. Raphael, P. S. Freedson, et al. (2006). Development of novel techniques to classify physical activity mode using accelerometers. *Medicine and science in sports and exercise* 38(9), 1626.
- Preece, S. J., J. Y. Goulermas, L. P. Kenney, and D. Howard (2009). A comparison of feature extraction methods for the classification of dynamic activities from accelerometer data. *IEEE Transactions on Biomedical Engineering* 56(3), 871–879.
- Preece, S. J., J. Y. Goulermas, L. P. Kenney, D. Howard, K. Meijer, and R. Crompton (2009). Activity identification using body-mounted sensors—a review of classification techniques. *Physiological measurement* 30(4), R1.

- Pruitt, L. A., N. W. Glynn, A. C. King, J. M. Guralnik, E. K. Aiken, G. Miller, and W. L. Haskell (2008). Use of accelerometry to measure physical activity in older adults at risk for mobility disability. *Journal of aging and physical activity* 16(4), 416.
- Ramsay, J. O. and B. W. Silverman (2006). *Functional data analysis*. Wiley Online Library.
- Randolph, T. W., J. Harezlak, and Z. Feng (2012). Structured penalties for functional linear models—partially empirical eigenvectors for regression. *Electronic journal of statistics* 6, 323.
- Ravi, N., N. Dandekar, P. Mysore, and M. L. Littman (2005). Activity recognition from accelerometer data. In *Aaai*, Volume 5, pp. 1541–1546.
- Reuter, I., S. Mehnert, P. Leone, M. Kaps, M. Oechsner, and M. Engelhardt (2011). Effects of a flexibility and relaxation programme, walking, and nordic walking on parkinson’s disease. *Journal of aging research* 2011.
- Richardson, C. A., N. W. Glynn, L. G. Ferrucci, and D. C. Mackey (2014). Walking energetics, fatigability, and fatigue in older adults: the study of energy and aging pilot. *The Journals of Gerontology Series A: Biological Sciences and Medical Sciences*, glu146.
- RStudio Team (2015). *RStudio: Integrated Development Environment for R*. Boston, MA: RStudio, Inc.
- Ruppert, D., M. P. Wand, and R. J. Carroll (2003). *Semiparametric regression*. Number 12. Cambridge university press.

- Sandroff, B. M., R. W. Motl, and Y. Suh (2012). Accelerometer output and its association with energy expenditure in persons with multiple sclerosis. *Journal of rehabilitation research and development* 49(3), 467.
- Schrack, J. A., V. Zipunnikov, J. Goldsmith, J. Bai, E. M. Simonsick, C. Crainiceanu, and L. Ferrucci (2013). Assessing the “physical cliff”: detailed quantification of age-related differences in daily patterns of physical activity. *The Journals of Gerontology Series A: Biological Sciences and Medical Sciences*, glt199.
- Sejdić, E., I. Djurović, and J. Jiang (2009). Time–frequency feature representation using energy concentration: An overview of recent advances. *Digital Signal Processing* 19(1), 153–183.
- Sekine, M., T. Tamura, T. Fujimoto, and Y. Fukui (2000). Classification of walking pattern using acceleration waveform in elderly people. In *Engineering in Medicine and Biology Society, 2000. Proceedings of the 22nd Annual International Conference of the IEEE*, Volume 2, pp. 1356–1359. IEEE.
- Sekine, M., T. Tamura, T. Togawa, and Y. Fukui (2000). Classification of waist-acceleration signals in a continuous walking record. *Medical engineering & physics* 22(4), 285–291.
- Simonsick, E. M., E. Fan, and J. L. Fleg (2006). Estimating cardiorespiratory fitness in well-functioning older adults: treadmill validation of the long distance corridor walk. *Journal of the American Geriatrics Society* 54(1), 127–132.
- Simonsick, E. M., P. S. Montgomery, A. B. Newman, D. C. Bauer, and T. Harris

- (2001). Measuring fitness in healthy older adults: the health abc long distance corridor walk. *Journal of the American Geriatrics Society* 49(11), 1544–1548.
- Strackiewicz, M., J. Urbanek, W. Fadel, C. Crainiceanu, and J. Harezlak (2016). Automatic car driving detection using raw accelerometry data. *Physiological Measurement* 37(10), 1757.
- Therneau, T. and B. Atkinson (2015). An introduction to recursive partitioning using the rpart routines. Mayo Foundation: Rochester, MN.
- Therneau, T., B. Atkinson, and B. Ripley (2015). *rpart: Recursive Partitioning and Regression Trees*. R package version 4.1-10.
- Troiano, R. P., D. Berrigan, K. W. Dodd, L. C. Masse, T. Tilert, M. McDowell, et al. (2008). Physical activity in the united states measured by accelerometer. *Medicine and science in sports and exercise* 40(1), 181.
- Urbanek, J. K., V. Zipunnikov, T. Harris, W. Fadel, N. Glynn, A. Koster, P. Caserotti, C. Crainiceanu, and J. Harezlak (2015). Prediction of sustained harmonic walking in the free-living environment using raw accelerometry data. *arXiv preprint arXiv:1505.04066*.
- Veltink, P. H., H. J. Bussmann, W. De Vries, W. J. Martens, and R. C. Van Lummel (1996). Detection of static and dynamic activities using uniaxial accelerometers. *IEEE Transactions on Rehabilitation Engineering* 4(4), 375–385.
- Welk, G. J., S. N. Blair, K. Wood, S. Jones, and R. W. Thompson (2000). A comparative evaluation of three accelerometry-based physical activity monitors. *Medicine and science in sports and exercise* 32(9; SUPP/1), S489–S497.

- Xiao, L., B. He, A. Koster, P. Caserotti, B. Lange-Maia, N. W. Glynn, T. B. Harris, and C. M. Crainiceanu (2016). Movement prediction using accelerometers in a human population. *Biometrics* 72(2), 513–524.
- Yang, C.-C. and Y.-L. Hsu (2010). A review of accelerometry-based wearable motion detectors for physical activity monitoring. *Sensors* 10(8), 7772–7788.
- Zhang, S., A. V. Rowlands, P. Murray, T. L. Hurst, et al. (2012). *Physical activity classification using the GENEa wrist-worn accelerometer*. Ph. D. thesis, Lippincott Williams and Wilkins.
- Zhang, T., J. Wang, L. Xu, and P. Liu (2006). Fall detection by wearable sensor and one-class svm algorithm. In *Intelligent computing in signal processing and pattern recognition*, pp. 858–863. Springer.

CURRICULUM VITAE

William Farris Fadel

EDUCATION

- Ph.D. in Biostatistics, Minor in Epidemiology, Indiana University, Indianapolis, IN, 2017
- M.S. in Statistics, Miami University, Oxford, OH 2007
- B.S. in Mathematics and Statistics, Miami University, Oxford, OH 2005

WORKING EXPERIENCE

- Research Assistant, Department of Biostatistics, Indiana University, Indianapolis, IN, July 2013 - June 2015
- Associate Instructor, Richard M. Fairbanks School of Public Health, Indiana University, Indianapolis, IN, July 2012 - June 2013
- Instructor, Department of Statistics, Miami University, Oxford, OH, August 2007 - May 2010
- Research Statistician I, Constella Group LLC, Cincinnati, OH, May 2006 - August 2006

HONORS AND AWARDS

- National Institutes of Health CTSA-TL1 award, Indiana University, Indianapolis, IN, 2010 - 2012

SELECTED PUBLICATIONS

- Strackiewicz, M., Urbanek, J., Fadel, W., Crainiceanu, C., and Harezlak, J. (2016). Automatic car driving detection using raw accelerometry data. *Physiological Measurement*, 37(10), 1757.
- Urbanek, J., Zipunnikov, V., Harris, T., Fadel, W., Glynn, N., Koster, A., Caserotti, P., Crainiceanu, C., and Harezlak, J. (2015). Prediction of sustained harmonic walking in the free-living environment using raw accelerometry data. arXiv preprint arXiv:1505.04066.
- Khan, B., Fadel, W., Tricker, J., Carlos, W., Farber, M., Hui, S., Campbell, N., Ely, E., and Boustani, M. (2014). Effectiveness of implementing a wake up and breathe program on sedation and delirium in the ICU. *Critical care medicine*, 42(12), e791-e795.